ABSTRACT

EL-HAGGAN, OMAR SHERIF. Evaluation of Rutting Behavior of Density Deficient Asphalt Mixtures. (Under the direction of Dr. Y. Richard Kim.)

The purpose of this research has been to evaluate the effect of change in density on the rutting performance of the asphalt pavement. This investigation helps in determining the appropriate penalty for density deficient pavements based on the rutting performance. Permanent deformation tests were performed at 30°, 40°, and 50°C on specimens with four different air void contents: 8, 8.75, 9.5, and 11%. More permanent deformation was observed at higher air voids and temperature. Complex modulus tests were also performed at the same four air void contents. Results showed that dynamic modulus decreases with the increase of both temperature and air void content as the asphalt mixture becomes softer at higher temperatures and air voids. Finally, a case study was performed to see the effect of air voids on the rutting behavior of the asphalt pavement. In this case study, the yearly rut depth for a certain pavement structure was predicted for both 8% and 11% air voids. Rut depth was determined to be 0.0074 inches for the 8% air voids pavement and 0.0168 inches for the 11% air voids pavement. This means that the pavement with 3% deficiency in air voids had an amount of rutting which is 2.3 times that of the in-specification pavement.

EVALUATION OF RUTTING BEHAVIOR OF DENSITY DEFICIENT ASPHALT MIXTURES

by

OMAR EL-HAGGAN

A Thesis submitted to the Graduate Faculty of
North Carolina State University
in partial fulfillment of the
requirements for the Degree of
Master of Science

CIVIL ENGINEERING

RALEIGH

2003

APPROVED BY:

____________________________ ____________________________

____

Chair of Advisory Committee

October 24, 2003

DEDICATION

It is my pleasure to dedicate this thesis to my beloved parents for the love and support they showed to me throughout the two years of my studies towards the Master of Science degree.

BIOGRAPHY

Omar El-Haggan was born in London, England in September 3, 1979. He moved to Kuwait in year 1981 and spent his childhood over there. In year 1990, he moved to Egypt with his family. He entered the American University in Cairo in year 1996, and received a Bachelor of Science degree with major in construction engineering and management in year 2001. After that, he came to the United States and enrolled in North Carolina State University in the civil engineering department, where he pursued his graduate studies towards the Master of Science degree. He worked as a graduate teaching assistant and then as a graduate research assistant under the supervision of Dr. Y. Richard Kim. In year 2003, he has been awarded his Master of Science degree in civil engineering.

ACKNOWLEDGEMENTS

First of all, I thank ALLAH for his aid and guidance.

I would like to extend a sincere appreciation and gratitude for my advisor, Dr. Y. Richard Kim for his encouragement and technical guidance. I would also like to thank all the research group members who helped me in my research work. Special thanks to Dr. Ghassan Chehab, Youngguk Seo, Yanqing Zhao, Mark King, Shane Underwood, Liza Runey, and Mostafa Momen for their help to me in both my experimental and analytical work. I would also like to thank North Carolina Department of Transportation for their sponsorship of this research. Finally, I feel very grateful to the spiritual support of my father, my mother, my sister Doaa, and my brother Mohammad.

TABLE OF CONTENTS

LIST OF TABLES

TABLE Page

LIST OF FIGURES

FIGURE Page

1. INTRODUCTION

1.1 Research Needs

North Carolina Department of Transportation (NCDOT) Standard Specifications for Road and Structures provide guidance on price adjustments for asphalt pavements that are not within reasonably close conformity with the specifications in terms of in-situ density but for which the work is accepted. Article 609-9 of the NCDOT Specifications for Road and Structures includes a formula that calculates the reduction in payment due to density deficiency. This formula is based on the assumption of a 50% price reduction for 3% deficiency in pavement density. These price adjustments were not developed based on the asphalt pavement performance and there is no supporting data for this relationship. Therefore, there is a need to determine the performance of asphalt pavement with deficient densities in order to know whether or not the price adjustments are adequate. If price adjustments are found to be inadequate, then a change in the standard specifications may occur and new price adjustments can be determined based on the performance of the asphalt pavement. This will give NCDOT a strong defense against the challenges from the contractors regarding the price reductions (Kim, 2001).

1.2 Research Objectives

The research presented herein was conducted as part of the NCDOT research project HWY-2002-07 entitled "Impact of Price Reductions on The Long-Term Pavement Performance of HMA Mixes in North Carolina". The objective of this research project is to determine whether price reductions described in Article 609-9 of the

NCDOT Specifications for Road and Structures is adequate based on economic analysis, and to develop a new recommendation for the price reduction methodology if the current policy is found to be inadequate. The objective of the research presented in this thesis is to determine the effect of change in pavement density on the rutting behavior of the pavement. This investigation will help in achieving the overall project objective by determining the appropriate penalty for density deficient pavements based on the rutting performance.

1.3 Research Approach

An essential element in assessing the impact of pavement construction deficiency on the service life is the correct prediction of the pavement response for known material properties and in-situ conditions. While this is a complex task, it can be accomplished through certain simplifications and assumptions that are deemed reasonable based on the information available in the literature and will not significantly compromise the accuracy of the predictions.

The framework adopted to predict the service life of a pavement for a given distress (fatigue or rutting) includes a laboratory testing program aimed at determining material properties and performance parameters needed in relating the pavement properties (structure and materials) to the service life of the pavement. Once those parameters are determined, they are applied to given inputs provided by the user for particular pavement conditions (category, structure, climate division, mixture type/properties if available, traffic, and percent density deficiency) to predict the pavement service life. The pavement service life will be governed by either fatigue or permanent deformation failure, whichever occurs first. Order of occurrence will ultimately depend on pavement category and structure, mixture properties, climate, and traffic conditions. The aforementioned procedure will be assembled as a computer application where the user simply provides the needed inputs. If some inputs are not available, such as coefficients in the rutting model, default values selected from a database would alternatively be used.

The following section outlines the framework used in predicting service life with regard to permanent deformation failure. The flowchart presented in Figure 1 provides an illustrative description of the prediction approach.

Triaxial compression permanent deformation testing is performed on commonly used two mixes, a surface course mix (S9.5C) and an intermediate course mix (I19C) for four different air voids and three different temperatures. The test results are used to determine the coefficients of the following rutting performance model that has been adopted in the 2002 AASHTO Design Guide:

$$\frac{\varepsilon_{pn}}{\varepsilon_r} = (\frac{ab}{\varepsilon_r})N^{b-1} \qquad (1)$$

where "a" and "b" are the regression constants determined from the power relationship between permanent strain (ε_p) and the number of load applications (N) (i.e., $\varepsilon_p = aN^b$), ε_{pn} is the incremental permanent strain, ε_r is the resilient strain, and *N* is the number of load applications. The model coefficients are determined for both surface course and intermediate course mixes as a function of both temperature and air voids. In addition to the permanent strain model, the inputs that are needed for the analysis are the climatic region, the road category which determines traffic volume and growth rate, the thicknesses, moduli and air void contents of both surface and intermediate courses, and the thicknesses and moduli of unbound layer materials including aggregate base and subgrade.

In this prediction algorithm, the smallest analysis period is the group of several hours in a day during which the traffic volume and temperature are relatively constant. The prediction approach accounts for the changes in temperature and loading rate along the depth of the asphalt layer. Therefore, each asphalt layer is divided into sublayers. For a particular day, the mid-depth temperatures of sublayers in both surface and intermediate layers are predicted using the temperature prediction program developed from the previous NCDOT project entitled “Statewide Calibration of Asphalt Temperature Study From 1992 And 1993”. This program allows the prediction of pavement temperature at any depth using the lowest and the highest air temperature of a day. Other inputs necessary to run this program have been established using the temperature database developed from the air and pavement depth temperatures, which were measured from different sites located in three climatic regions in North Carolina.

Another factor that influences the response of the asphalt layer is the loading rate. The loading rate under a moving load decreases as the depth increases. The changing loading rate along the depth is incorporated using the previous research result.

Once the temperature and the loading rate are determined, the dynamic modulus of each sublayer can be obtained from the dynamic modulus mastercurve based on the sublayer temperature, loading rate and air void content. These moduli and unbound layer moduli are inputs to the pavement response model to determine the compressive strain in the middle of each subalyer. This compressive strain is used as the resilient strain. Also, the regression coefficients “a” and “b” in Eq. (1) are determined for each sublayer from both the mid-depth temperature and the air void content of the layer. Finally, the permanent strain is calculated from Eq. (1) using the regression constants, resilient strain, and the ESALs for a given analysis period. Rut depth is determined by adding permanent deformations in sublayers, which are calculated by multiplying permanent strain and sublayer thickness.

The process described above is applied to different analysis periods of a day. Rut depths determined from all the analysis periods are added together to obtain the daily rut depth. The same procedure is repeated for the subsequent days. For each day, the temperature will change, thus yielding different regression constants and different plastic strain, and therefore different rut depths. At the end, all the daily rut depths are summed to get the total yearly rut depth of the pavement. For the subsequent year, the same calculations are again repeated, except that the ESALs will change due to the traffic growth. The procedure is repeated until the cumulative rut depth for all years exceeds the maximum allowable surface rut depth. The rut depth of 0.25 inch is used in this study as the failure criterion. Using this analysis method, service life will be determined for both the standard and deficient air void pavements. The price reduction will be determined for the deficient pavement by comparing its service life to that when no deficiency in air voids is present.

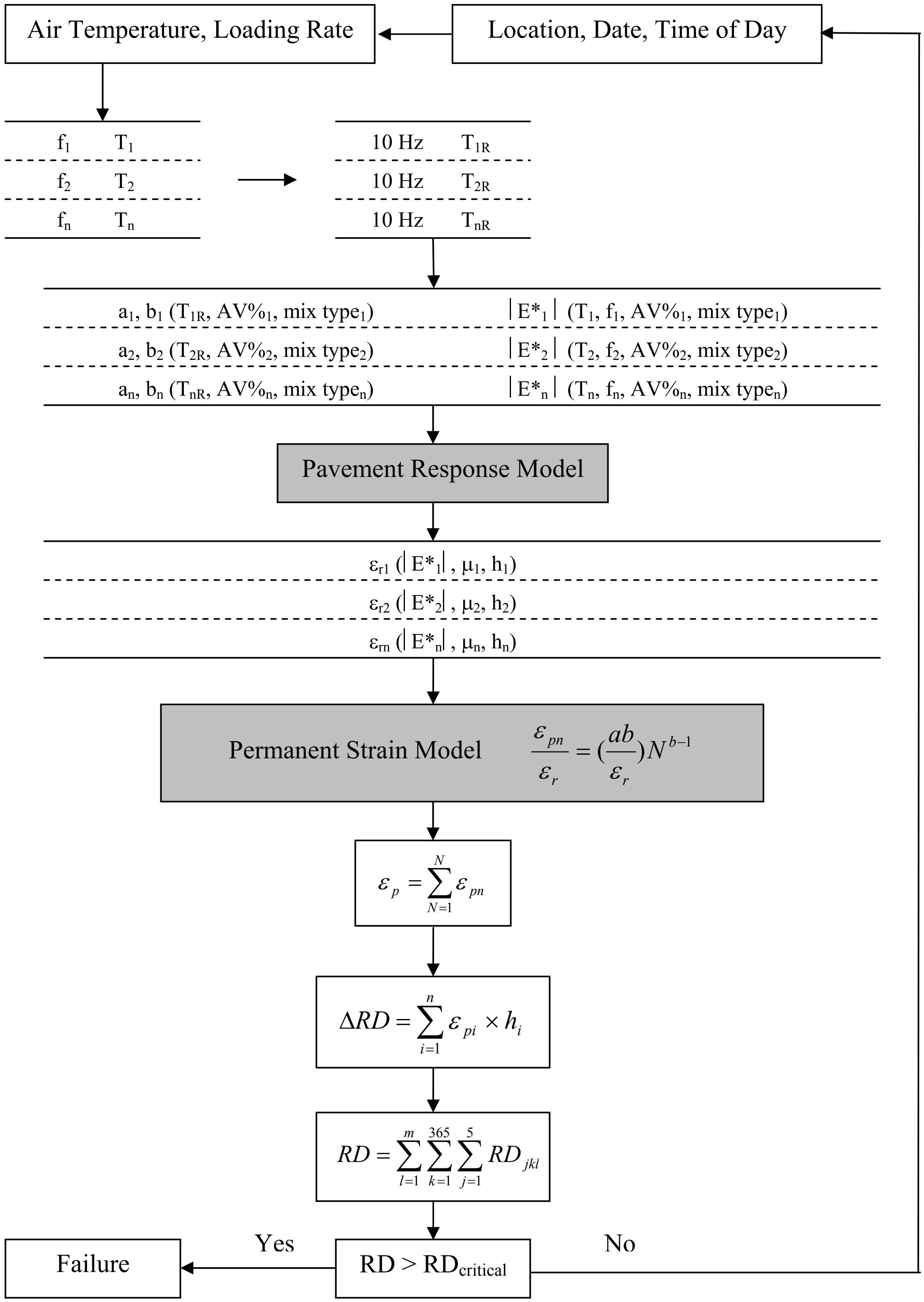

Figure 1. Framework for Prediction of Rutting Life

Definitions:

- T: Temperature
- f: Loading rate
- AV%: Air voids in percentage
- h: Thickness
- μ: Poisson's ratio
- $|E^*|$: Dynamic modulus
- a, b: Permanent deformation regression coefficients
- ε_r : Resilient strain
- ε_{pn}: Incremental permanent strain due to a single load application
- ε_p: Total permanent strain
- N: Number of load applications for a certain group of several hours
- n: Number of sublayers in the asphalt pavement
- RD: Rut Depth
- j: Several hours group index
- k: Day index
- l: Year index

1.4 Thesis Organization

This report is divided into five chapters. Chapter 1 contains the research needs, research objectives, research approach, and the thesis organization. Chapter 2 explains the theoretical background and literature review about rutting in asphalt pavements and permanent deformation for hot mix asphalt. Chapter 3 includes the descriptions of the materials used in the study, the specimen preparation methods, and the experimental program. Chapter 4 has the laboratory testing results and analysis, including complex modulus testing and repetitive permanent deformation testing. Examples on how the rutting predictive algorithm can be used are also presented in this chapter. Finally, Chapter 5 presents the conclusions that were made after conducting the testing and analysis for both standard and deficient air voids pavements. Field densification study and test protocols are included in the appendices.

2. THEORETICAL BACKGROUND AND LITERATURE REVIEW

2.1 Rutting in Asphalt Pavements

Rutting is defined as surface deformation under the wheel paths. It stems from the permanent deformation in any of the pavement layers or the subgrade. There are two main types of rutting. The first one is rutting in asphalt layer, and the other is rutting in subgrade or base. Most of rutting in today's pavements is due to the permanent deformation in the asphalt layer. Rutting is considered to be one of the important distresses in the pavement since significant rutting can lead to major structural failures and hydroplaning potentials.

The amount of permanent deformation in the asphalt pavement depends on many factors such as the stress state, frequency of the loading, duration of unloading (rest period), number of cycles applied to the pavement, confining stress, air void content of the asphalt concrete mix, aging of the binder, moisture, and pavement temperature.

Rutting studies in the field (Kaloush and Witczak, 2002) have shown that two phases of rutting can develop in the asphalt concrete pavement. The first kind is structurally related and is due to the accumulation of the permanent deformation in the vertical direction within the pavement layers under traffic loads. Part of the rutting in this first phase is also due to post construction densification. The second phase is more critical to the stability of the mixture and is shear stress related. Shear ruts occur due to the lateral deformation of material within the pavement layer. This second phase is called shear deformation or plastic flow, and it may or may not occur in the pavement.

2.2 Triaxial Repetitive Permanent Deformation Testing

Performance based tests are tests that measure material properties which can be used in a fundamental response model in order to predict mixture response to various loadings and environmental conditions. Performance based test methods are categorized by the type of the test, type of load application, and type of load pulse. There are different types of performance based tests. One of them is the repeated load permanent deformation test. In this case, the type of test is triaxial compressive, the type of load application is repetitive load, and the type of load pulse is haversine.

In order to provide realistic and accurate relationships between laboratory performance and actual performance in the field, it is important to conduct laboratory tests under the same stress conditions and environmental conditions of the field. Three factors have to be considered:

1. Climatic conditions: For asphalt concrete, temperature is the primary factor to be considered
2. Traffic level: Both the number of load repetitions and the rate of loading are important
3. Stress levels: It is important to simulate the triaxial state of stress in the asphalt layer

All these factors have to be considered for any performance test in order to be able to simulate the pavement conditions in the field (Kaloush, 2001).

The triaxial compression repeated load test is one of the test methods in which these factors can be included. This test employs a repetitive haversine load with a rest period and records the cumulative permanent deformation as a function of the number of load cycles over the test period. Typically, a haversine pulse load of 0.1 second and 0.9 second rest time is applied.

2.3 Incremental Permanent Strain Model

From the triaxial repetitive permanent deformation test, permanent deformation response of asphalt concrete under cyclic loading can be obtained. Figures 2 and 3 show the typical relationship between the total cumulative plastic strain and the number of load cycles in normal and log-log scales, respectively. In Figure 3, three zones are defined along the cumulative permanent strain curve: primary, secondary, and tertiary. In the primary zone, permanent deformations accumulate rapidly as can be seen in Figure 2. During the secondary zone, the incremental permanent deformations decrease reaching a constant value. Finally, the incremental permanent deformations again increase and permanent deformations accumulate rapidly in the tertiary zone. The cycle number at which tertiary flow starts is referred to as the "Flow Number". It is important to note that well performing mixes stay in the secondary zone and do not show any tertiary flow in normal loading conditions under standard axle loads (Kaloush and Witczak, 2002).

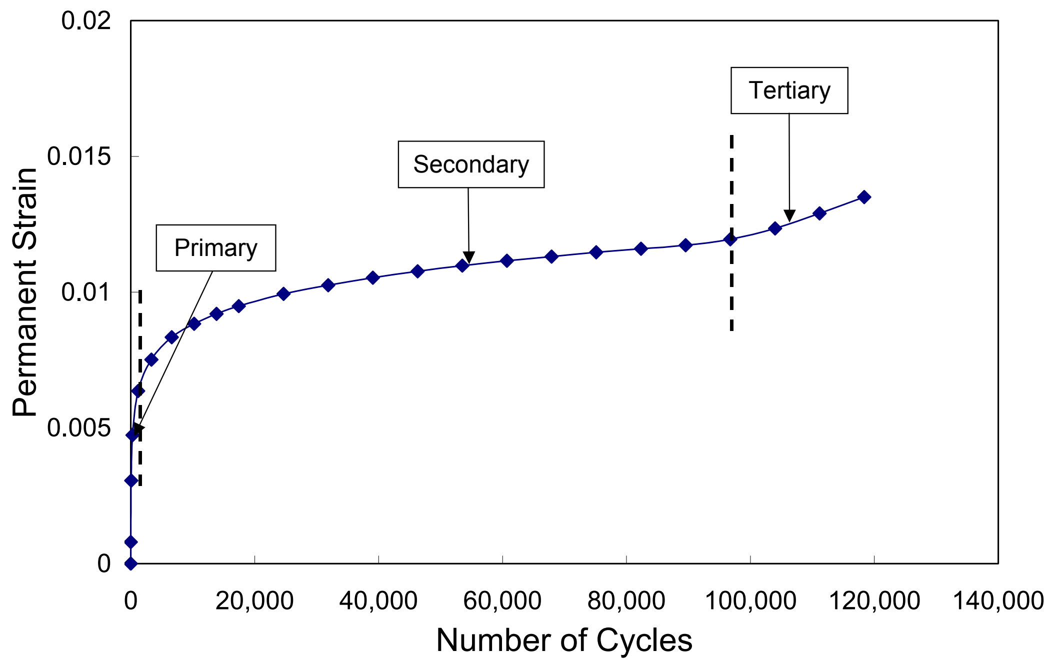

Figure 2. Typical Relationship Between Total Cumulative Plastic Strain and Number of Load Cycles

The linear portion in the middle of the curve in Figure 3 is used to represent the permanent strain response of a mix. This portion can be expressed by the following classical power model:

$$\varepsilon_p = aN^b \tag{2}$$

where "a" and "b" are regression constants. The intercept "a" represents the permanent strain at N = 1. The slope "b" represents the rate of change in log (ε_p) as a function of the change in log (N). An alternative form of the mathematical model used to characterize the plastic strain per load repetition (ε_{pn}) relationship can be expressed by:

$$\frac{\partial \varepsilon_p}{\partial N} = \varepsilon_{pn} = \frac{\partial (aN^b)}{\partial N} \tag{3}$$

Or

$$\varepsilon_{pn} = abN^{(b-1)} \tag{4}$$

The resilient strain (ε_r) is assumed to be independent of the load repetition value (N). As a result, the ratio of plastic to resilient strain components of the material can be defined by:

$$\frac{\varepsilon_{pn}}{\varepsilon_r} = (\frac{ab}{\varepsilon_r})N^{b-1} \tag{5}$$

Letting: $\mu = \frac{ab}{\varepsilon_r}$ and $\alpha = 1 - b$ one obtains:

$$\frac{\varepsilon_{pn}}{\varepsilon_r} = \mu N^{-\alpha} \tag{6}$$

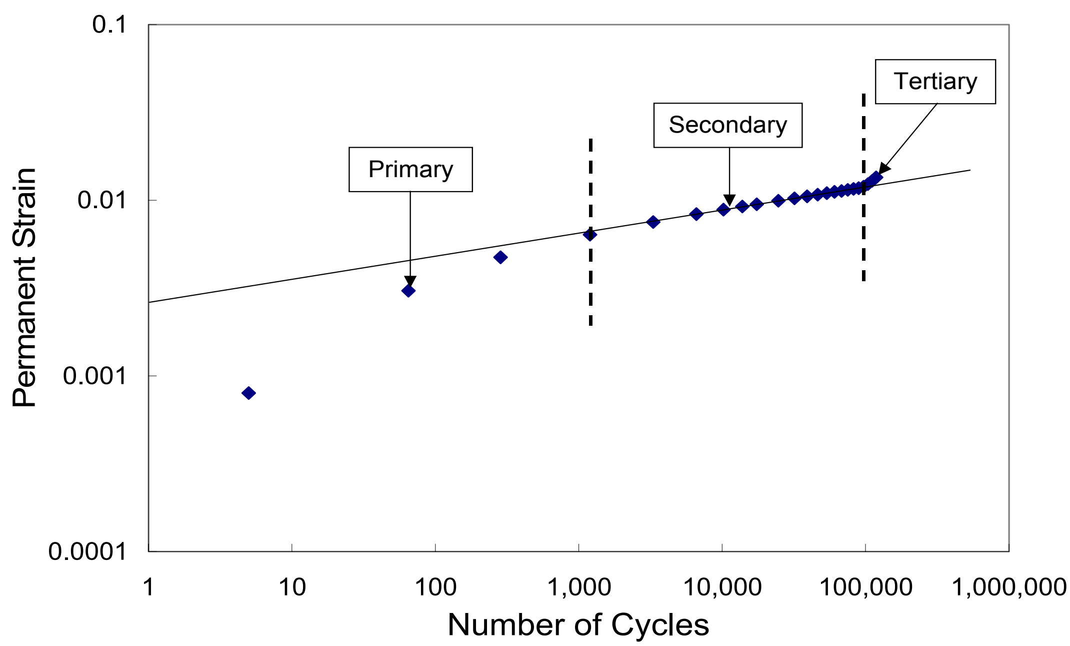

Figure 3. Regression Constants “a” and “b” When Plotted on a Log-Log Scale

where ε_{pn} is the permanent strain due to a single load application; i.e., at the N^{th} application. The coefficient μ is the permanent deformation parameter representing the constant of proportionality between permanent strain and elastic strain. The exponent α is a permanent deformation parameter indicating the rate of decrease in incremental permanent deformation as the number of load applications increases.

2.4 Background on Testing Conditions

Several researches were done on permanent deformation testing, and different testing conditions were used. In this section, some of the testing conditions are presented. These testing conditions include testing temperature, deviator stress level, and confining stress level.

According to the draft test protocol for the simple performance test for permanent deformation based upon repeated load test of asphalt concrete mixtures, the effective pavement temperature covers approximately the temperature range of 25 to 60°C. The deviator stress level covers the range of 10 to 30 psi for the unconfined tests and 70 to 140 psi for the confined tests. The confining stress ranges between 5 and 30 psi.

Brown and Cooper used a temperature of 40°C for their test, and their test was conducted under a confining stress of 14.4 psi (Brown and Cooper, 1984). Kaloush and Witczak (2002) used different testing conditions for different mixtures. For MnRoad mixtures, they used two temperatures of 37.8°C and 54.4°C. In the case of 37.8°C temperature, the deviator stress level was 30 psi, while in the case of 54.4°C temperature, two deviator stress levels of 10 and 30 psi were used. Deviator stress levels were low for MnRoad tests since all the tests were unconfined. For ALF mixtures, the testing temperature was 54.4°C. Unconfined tests were performed at two deviator stress levels of 10 and 20 psi, and confined tests were performed at 140 psi deviator stress and 20 psi confining stress. As for WesTrack mixtures, the testing temperature was also 54.4°C. Unconfined tests were conducted at a deviator stress of 10 psi, and confined tests were conducted at 140 psi deviator stress and 20 psi confining stress (Kaloush and Witczak, 2002).

3. SPECIMEN PREPARATION AND EXPERIMENTAL PROGRAM

3.1 Specimen Preparation

3.1.1 Asphalt Concrete Mixtures

Two mixture types were used in this study: I19C which is an intermediate course mix, and S9.5C which is a surface course mix. These two mixes are the most commonly used mixtures in asphalt pavement construction in North Carolina.

I19C:

For I19C mix, the aggregate type is granite. The source of the aggregate is Martin-Marietta Garner quarry. The properties of different stockpiles are as follows:

Material	Blend %
Coarse aggregate, #57	21
Coarse aggregate, #78M	49
Screenings, Dry	20
Screenings, Washed	10

The asphalt binder for this mixture is PG 64-22. The total binder percentage in the mix is 4.7%. The binder includes 0.5% anti-strip additive. The mixing temperature is 158°C and the compaction temperature is 145°C. The maximum specific gravity (G_{mm}) was measured to be 2.464.

S9.5C:

The same aggregate used in I19C was used in making S9.5C specimens. The properties of different stockpiles are as follows:

Material	Blend %
Coarse aggregate, #78M	46
Screenings, Washed	16
Screenings, Regular	30
Sand, Pit	8

The asphalt binder for this mixture is PG 70-22. The total binder percentage in the mix is 5.2%. The binder includes 0.5% anti-strip additive. The mixing temperature is 166°C and the compaction temperature is 155°C. The maximum specific gravity (G_{mm}) was measured to be 2.469.

3.1.2 Determination of Target Air Voids for Permanent Deformation Testing

In this study, specimens with air voids outside of the specification were tested and compared with the results from specimens within the specification in order to determine the effect of change in density on the rutting performance of the pavement. The NCDOT specification calls for minimum 92% of maximum specific gravity (G_{mm}). Since the density is based on G_{mm}, then air void content can be calculated by subtracting the percent density from 100. Thus, 92% density represents the mix with 8% air void content. Three percent deficiency in density means 89% density and therefore 11% air voids. The deficiencies in air voids that were tested in this project were 0, 0.75, 1.5, and 3 %, which correspond to initial air void contents in the field pavement of 8, 8.75, 9.5, and 11 %.

In the triaxial repetitive permanent deformation test, it is believed that the target air void contents to be used for the laboratory specimens should be the same as the initial air void contents observed in actual pavements. This belief stems from the fact that rutting in the field is due to two different mechanisms. The first type is densification which occurs due to the reduction in air voids volume only. This type of rutting occurs in the early part of the pavement's service life. The other type is plastic flow (shear deformation) in which consolidation occurs due to reduction of the total voids in the mineral aggregates. Pavement performance studies show that when the air voids reduce to less than 3%, it is the plastic flow mechanism which predominates. Since both of these mechanisms contribute to the rutting of pavements, it is important to capture these mechanisms in the laboratory test setting. Therefore, the target air void contents for the laboratory triaxial permanent deformation testing were selected to be the same as the initial air void contents in the field, i.e., 8, 8.75, 9.5, and 11%. The complete air void reduction study is presented in Appendix A.

3.1.3 Specimen Fabrication

Gyratory specimens were prepared to 178 mm height and 150 mm diameter, and then were cored and cut to 150 mm height and 100 mm diameter. Specimens were fabricated to four different air void contents: 8, 8.75, 9.5, and 11%. Obtaining different air void contents was achieved by varying the total mass of the gyratory specimen. The relationship between the total mass of the gyratory specimen and the air voids of the tested specimen was determined for the two mixes and summarized in Table 1.

Table 1. Total Mass for the Required Air Void Contents

Air Voids (%)	**Total Mass (g)**	
	S9.5C	**I19C**
8	6,960	6,900
8.75	6,900	6,840
9.5	6,840	6,760
11	6,700	6,620

3.2 Experimental Program

3.2.1 Testing System

UTM-25, a servo-hydraulic universal testing machine, was used in testing. It was manufactured by Industrial Process Controls in Australia. It has a loading capacity of 25 KN, and it is capable of applying load over a wide range of frequencies ranging from 0.01 Hz to 25 Hz. UTM is fully computer controlled.

The temperature control system of UTM is refrigeration-based. It has a heating element to achieve high temperatures. The temperature control system was able to achieve the required testing temperatures ranging from -10°C to 50°C. An asphalt concrete dummy specimen with a temperature probe placed in the middle of the specimen was placed inside the triaxial cell in order to check the actual temperature of the specimen during testing.

The data acquisition system for UTM is also fully computer controlled and is capable of measuring and recording data from several channels simultaneously. Eleven channels were used in this particular testing: four for vertical LVDTs, four for radial LVDTs, one for load cell, one for actuator, and one for confining pressure. Data acquisition programs were prepared using LabView software for data collection and analysis.

The data for vertical and radial deformations were measured with linear variable differential transformers (LVDTs). The GTX 5000 spring-loaded LVDTs were used to measure redial deformations. Those LVDTs are used to maintain positive contact with the specimen throughout the test. Four LVDTs were spaced 90 degrees apart along the circumference and at mid-height of the specimen. Concerning the vertical deflection measurement, four CD 100 LVDTs were placed in the mid-portion of the specimen at 90 degrees apart in order to measure deflections for a specific gage length.

In this study, a gage length of 75 mm was used to measure the vertical strain in the middle of the specimen where the strain is relatively constant. However, in the particular tests of 11% air void content specimen at 50°C temperature, the strain was too high to be covered by CD LVDTs range. Therefore, the displacement measured by the UTM actuator (that has a much longer range than CD LVDTs) was evaluated as a substitute for the on-specimen LVDT measurements. The main concern over this substitute is the end effect and machine compliance, which may result in different strains when displacements are measured from the actuator and from on-specimen LVDTs.

Measurements from both the LVDTs and the actuator were analyzed and plotted in Figures 4 and 5. It can be seen that the strain calculated from the actuator displacement matches quite well with the strain calculated from the displacement measured by on-specimen LVDTs. This agreement suggests firstly that machine compliance was not a significant factor and, secondly, that the end effect was minimal. The first observation is reasonable because the stiffness of the asphalt specimen at the test temperature of 50°C was much lower than the stiffness of the machine and parts in the testing apparatus. Also, the silicon grease lubrication and the use of two rubber membranes seemed to work quite well in minimizing the end effect. Consequently, it was decided to use the actuator measurement in cases where vertical deformation is too high for the on-specimen LVDTs to cover.

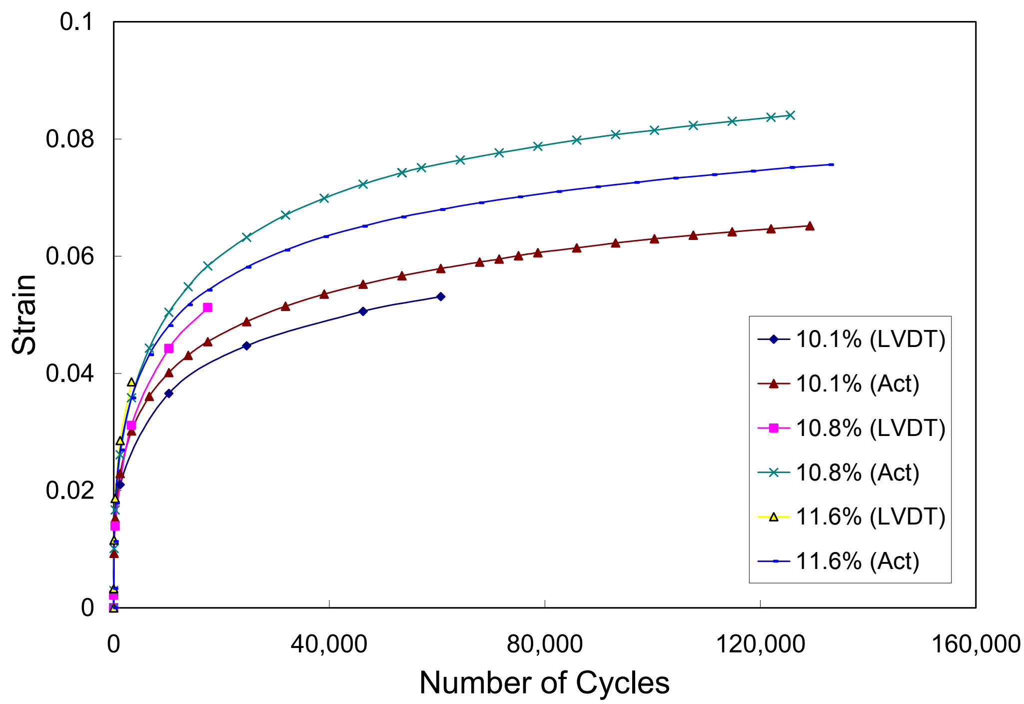

Figure 4. LVDTs Measurement vs. Actuator Measurement (S9.5C)

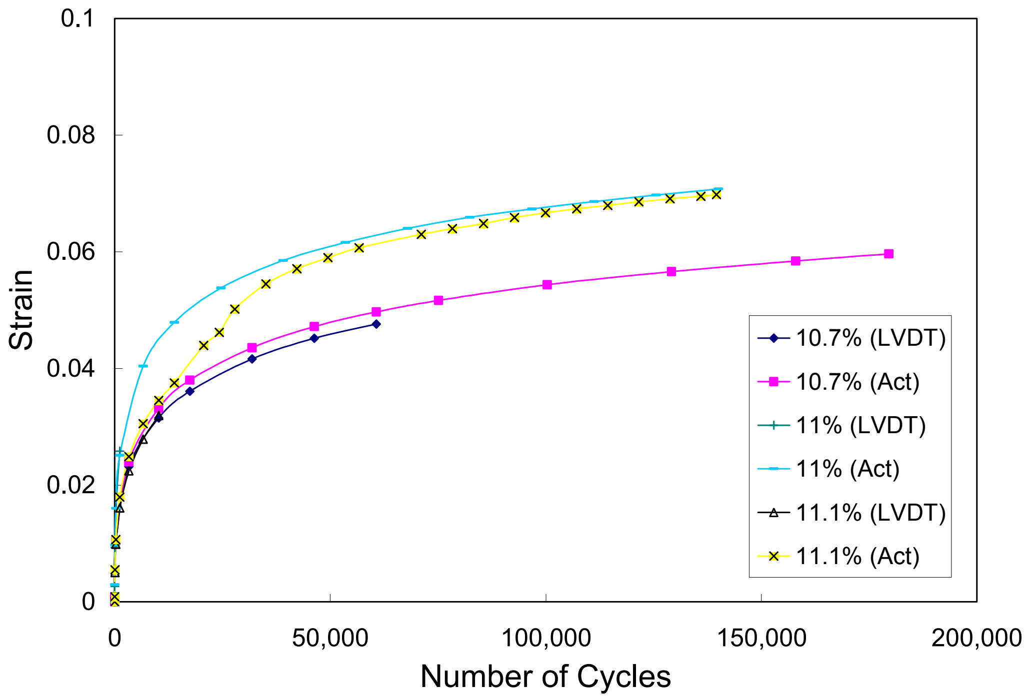

Figure 5. LVDTs Measurement vs. Actuator Measurement (I19C)

3.2.2 Determination of Testing Temperatures

The effective temperature for permanent deformation, T_{eff} (PD), is defined as a single test temperature at which the amount of permanent deformation accumulated would be equivalent to that which could be measured by considering the seasonal fluctuation of temperature throughout the year. In this study, the effective temperature was calculated in order to determine the testing temperature. The effective temperature was calculated for each of the eight climatic regions in North Carolina. These climatic regions are shown in Figure 6.

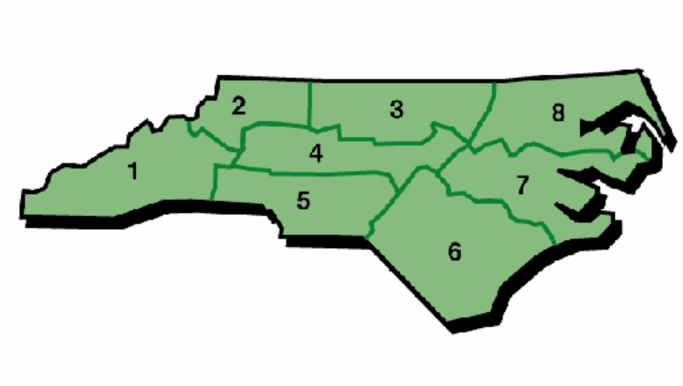

Figure 6. The Eight Climatic Regions of the State of North Carolina

Temperature data was obtained from the National Climatic Data Center. For each region, the average monthly temperature was obtained for every year from 1895 until 2001. Then, the annual temperature was calculated for each year as the average of the temperatures of the 12 months. Finally, the effective temperature was calculated for each climatic region using Witczak's equation shown below (Cominsky, 1994):

$$T_{eff}\,(PD) = 30.8 - 0.12\, Z_{cr} + 0.92\, MAAT_{design} \qquad (7)$$

where T_{eff} (PD) = effective temperature in °C for permanent deformation,

Z_{cr} = critical depth within the mix layer in question in mm, and

$MAAT_{design} = MAAT_{average} + K_{\alpha}\, \sigma_{MAAT}$

where $MAAT_{average}$ = average annual air temperature in °C (computed as the average of all the annual temperatures from year 1895 till year 2001),

σ_{MAAT} = standard deviation of the distribution of mean annual air temperature for the geographical location, and

K_α = value computed from normal probability tables related to the designer's selection of appropriate reliability level (R) desired for the project. A 99% probability was selected for this project. The value of K_α corresponding to 99% probability is 2.327.

The effective temperature is considered to be the mid-depth temperature of the asphalt concrete layer. Therefore, the critical depth is the depth from the surface to the mid-depth of the layer in question. The effective temperature was determined for both the surface course and intermediate course for two extreme cases. In the first case, the thickness of the surface layer was assumed to be 3.5 inches. Since rutting is assumed to occur mostly in the top 4 inches of the pavement, then the part that is exposed to rutting in the intermediate layer is only the top 0.5 inch of the layer. In this case, the critical depth was calculated as 1.75 inches for the surface layer and 3.75 inches for the intermediate layer. The effective temperatures corresponding to these depths are shown in Table 2. In the second case, the thickness of the surface layer was assumed to be only one inch. In this case, the part that is exposed to rutting in the intermediate layer is the top 3 inches of the layer. The critical depth is 0.5 inch for the surface layer and 2.5 inches for the intermediate layer in this case. The effective temperatures of the surface and intermediate layers for the eight regions were calculated for these two cases using Eq. (7) and tabulated in Table 2.

Table 2. Effective Temperatures (in °C) for the Eight Climatic Regions of North Carolina Corresponding to Different Cases

Surface course thickness	Layer	Region No.								Average
		1	2	3	4	5	6	7	8	
3.5 inches	Surface course	38.4	37.2	40.3	40.5	41.1	41.9	41.7	41.1	40.3
	Intermediate course	32.3	31.1	34.2	34.4	35.0	35.8	35.6	35.1	34.2
1 inch	Surface course	42.2	41.0	44.1	44.3	45.0	45.7	45.5	45.0	44.1
	Intermediate course	36.1	34.9	38.0	38.2	38.9	39.7	39.4	38.9	38.0

Since the effective temperature values range between 31.1°C and 45.7°C, the selected temperatures for permanent deformation testing are 30°, 40°, and 50°C. These three temperatures seem to cover the temperature ranges that may occur under various thickness and temperature combinations.

3.2.3 Determination of Testing Stress Levels

In order to perform permanent deformation prediction analyses, it is essential to determine the stresses in the pavement structure. Both deviator stress and confining stress need to be determined for laboratory testing purposes. As previously discussed in literature review, the deviator stress ranges between 70 to 140 psi in the case of confined tests. In this research, a statistical model developed by Hafez (Kaloush, 2001) was used to estimate the deviator stress in the asphalt layer. This model is able to estimate deviator stress for a given pavement structure, material quality, and tire pressure. The following is the equation for this model:

$$\sigma_d = -43.82 + 62.54E_{ac} + .0004E_{sg} + 0.585p_c + 14.78z_{cr} \qquad (8)$$

where:

σ_d = deviator stress, psi,

E_{ac} = asphalt layer modulus, 10^6 psi,

E_{sg} = subgrade modulus, psi,

p_c = tire pressure, psi, and

z_{cr} = depth within the asphalt layer, inches.

Moduli values were assumed to be 1,000 ksi for asphalt layer and 25 ksi for subgrade layer. Tire pressure was assumed to be 100 psi. Critical depth was assumed to be 2 inches. Then, Hafez model was applied using these values, and the deviator stress came out to be 116.8 psi. Consequently, it has been decided to use a deviator stress of 120 psi for all permanent deformation tests in this research.

As for confining pressure, it ranges between 5 and 30 psi according to the draft test protocol for the simple performance test for permanent deformation based upon repeated load test of asphalt concrete mixtures. Consequently, a confining stress of 20 psi was used for all permanent deformation tests in this project.

3.2.4 Test Methods and Number of Tests

The experimental program for this study consists of two series of testing, complex modulus and permanent deformation testing.

1) Complex Modulus Testing:

Complex modulus testing was performed for the construction of the linear viscoelastic (LVE) mastercurves for dynamic modulus |E*| and phase angle (ϕ). Two replicate tests were conducted on mixtures with 8, 8.75, 9.5, and 11% air void contents. The total number of complex modulus tests was 16 (4 air void contents, 2 replicates, 2 mixes). |E*| is needed to normalize the permanent deformation testing data to minimize the sample-to-sample variability, and is also needed in predicting resilient strains using the multi-layered elastic analysis.

Complex modulus testing was performed by applying sinusoidal loading in compression sufficient to produce total strain amplitude of about 50-60 micro-strains. Eight frequencies were applied at three different temperatures. The eight frequencies were 25, 10, 5, 1, 0.5, 0.1, 0.05, 0.01 Hz. The three temperatures were –10, 10, 35 °C. Before the complex modulus testing, a confining pressure of 20 psi was applied to the specimen. The radial deformation was monitored with the confining pressure and the complex modulus test was initiated after the radial strain is stabilized. Testing was conducted on temperatures starting from the lowest to the highest, and frequencies were applied at each temperature from the fastest to the slowest. Before applying the first frequency, preconditioning load was applied at 25 Hz. The load amplitude was adjusted based on the material stiffness, air void content, temperature, and frequency to keep the strain response within the 50-60 micro-strains. After each frequency, a five-minute rest period was allowed for the specimen recovery before the next frequency was applied. More details about the complex modulus testing procedures are presented in Appendix C.

Tables 3 and 4 include a summary of testing conditions for the complex modulus tests for the two mixes. For each case, there is a range of loads depending on the specimen stiffness and air void content.

Table 3. Complex Modulus Test Conditions (S9.5C)

Frequency (Hz)	Cycles	Load Range (KN)			Following Rest Period (sec)
		Temperature (C)			
		-10	10	35	
25 preconditioning	200	6.5-8	2.6-3.2	0.75-1	300
25	200	13-16	5.2-6.4	1.5-2	300
10	200	8-11.5	4.2-5.6	1.2-1.8	300
5	100	7.3-10.5	3.7-5.1	1-1.6	300
1	20	6.7-9.5	3.1-4.4	0.7-1.1	300
0.5	15	6.3-8.5	2.6-4	0.55-0.9	300
0.1	15	5.9-8	2-3.2	0.45-0.7	300
0.05	12	5.5-7.2	1.6-2.8	0.4-0.62	300
0.01	8	5.1-6.5	1.1-2.2	0.35-0.52	300

Table 4. Complex Modulus Test Conditions (I19C)

Frequency (Hz)	Cycles	Load Range (KN)			Following Rest Period (sec)
		Temperature (C)			
		-10	10	35	
25 preconditioning	200	7-10	2.9-4	0.8-1.1	300
25	200	14-20	5.8-8	1.6-2.2	300
10	200	10-14.5	5-7	1.2-1.9	300
5	100	9-13	4-6	1-1.6	300
1	20	8-11.5	3.2-5	0.7-1.2	300
0.5	15	7-10	2.5-4.2	0.55-1	300
0.1	15	6.4-9.2	2-3.4	0.45-0.85	300
0.05	12	5.8-8.5	1.5-3	0.4-0.75	300
0.01	8	5-7.5	1-1.7	0.35-0.6	300

2) Permanent Deformation Testing:

Permanent deformation testing was performed at three temperatures: 30°, 40°, and 50°C. For each of the three temperatures, two replicates were tested at four air void contents: 8, 8.75, 9.5, and 11%. The total number of permanent deformation tests was 48 (3 temperatures, 4 air void contents, 2 replicates, 2 mixes)

Triaxial repetitive permanent deformation tests were performed using a haversine pulse load of 0.1 second duration followed by a rest period of 0.9 second. Twenty psi confining pressure and 120 psi deviator stress were applied to simulate in situ stress conditions. All the tested specimens had the dimensions of 100 mm diameter and 150 mm height. Before the permanent deformation test starts, the complex modulus test was performed in order to obtain a fingerprint of the specimen being tested. This was done by applying 40 cycles at a frequency of 10 Hz. Load level was adjusted depending on the testing temperature in order to obtain 50-60 micro-strains. More details about the permanent deformation testing procedures are presented in Appendix B.

4. RESULTS AND ANALYSIS

4.1 Complex Modulus Testing

Master curves were developed from complex modulus testing on specimens with different air voids. The following is the sigmoidal function which was used in fitting each master curve:

$$Log|E^*| = a + \frac{b}{1 + \dfrac{1}{\exp^{d + e(\log f_R)}}} \qquad (9)$$

where,

$|E^*|$ = dynamic modulus (in MPa),

a, b, d, e = regression coefficients,

$f_R = f \times a_T$ = reduced frequency (in Hz),

f = frequency, and

a_T = shift factor.

Figures 7 and 8 show the master curves for different air voids specimens for both S9.5C and I19C mixes. For the two mixes, the sample-to-sample variation and similarity of the data from individual tests made it difficult to observe a clear effect of air voids on the dynamic modulus. Therefore, it was decided to plot the coefficients a, b, d, and e in Eq. (9) against the air void content as shown in Figures 9 and 10. Then, each of these coefficients was fitted against the air voids using a linear function. This function enables the user to obtain each of the four coefficients and then calculate dynamic modulus at any desired air void content. When the dynamic moduli were calculated at different air voids using this function, the effect of the air voids appeared as having a smaller dynamic modulus value as the air void content increased. This trend makes sense because the specimen becomes softer at higher air voids.

In addition, shift factors were plotted against temperature for each individual test. Then, all the shift factor versus temperature curves were plotted on one plot to demonstrate the effect of air voids on shift factors (Figures 11 and 12). As can be seen from these figures, the curves are close to each other and no clear pattern is found for the shift factor curves as a function of air void content. It was concluded that there is no significant effect of air voids on shift factors. Therefore, one representative curve of shift factor versus temperature was selected for each of the two mixes as shown in Figures 13 and 14.

Consequently, the a, b, d, and e coefficients are functions of air voids, and the shift factor is a function of temperature. Therefore, knowing the air void content of the asphalt layer, the values of the four coefficients can be determined which, in turn, define the sigmoidal function for the dynamic modulus. Also, knowing the temperature of the asphalt layer, the shift factor can be determined, and then the reduced frequency can be obtained by multiplying the shift factor by the loading frequency. Finally, the dynamic modulus of the asphalt layer can be calculated by inputting the reduced frequency into the sigmoidal function. The approach described above can be summarized by expressing the variables in the sigmoidal function as a function of air void content and temperature, as follows:

$$Log|E^*| = a(AV\%) + \frac{b(AV\%)}{1 + \dfrac{1}{\exp^{\{d(AV\%)+e(AV\%)\times \log f \times a_T(T)\}}}} \tag{10}$$

where the parenthesis after a, b, d, e and a_T indicates that these coefficients are functions of the variable inside the parenthesis.

The calculation of $|E^*|$ is useful in the following two areas:

1. Normalization of the permanent deformation test data: The permanent deformation test results were normalized to minimize the sample-to-sample variation. Normalization was performed by calculating the reference $|E^*|$ for each test based on the air voids of the specimen and temperature and comparing it to the actual $|E^*|$ of the specimen. This actual $|E^*|$ was determined by running a dynamic modulus test at a frequency of 10 Hz prior to the permanent deformation test at the test temperature to obtain a fingerprint of the specimen stiffness.

2. Pavement response calculation: The dynamic modulus of the asphalt layer is needed in the pavement response calculation using the multilayered elastic analysis.

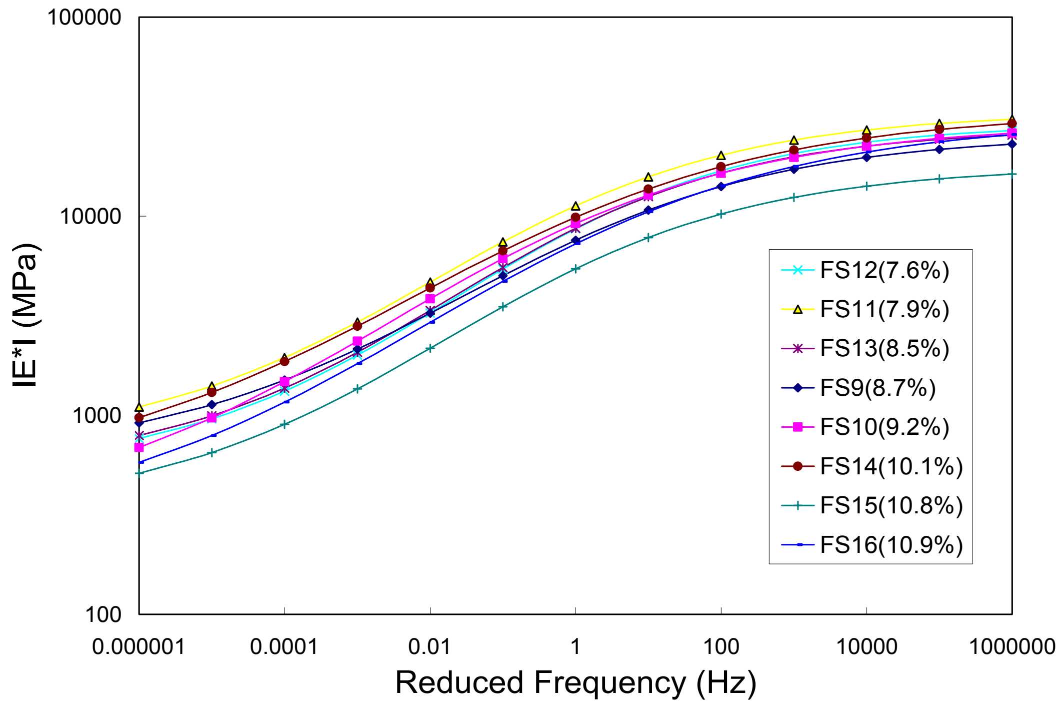

Figure 7. Effect of Air Void Content on |E*| (S9.5C)

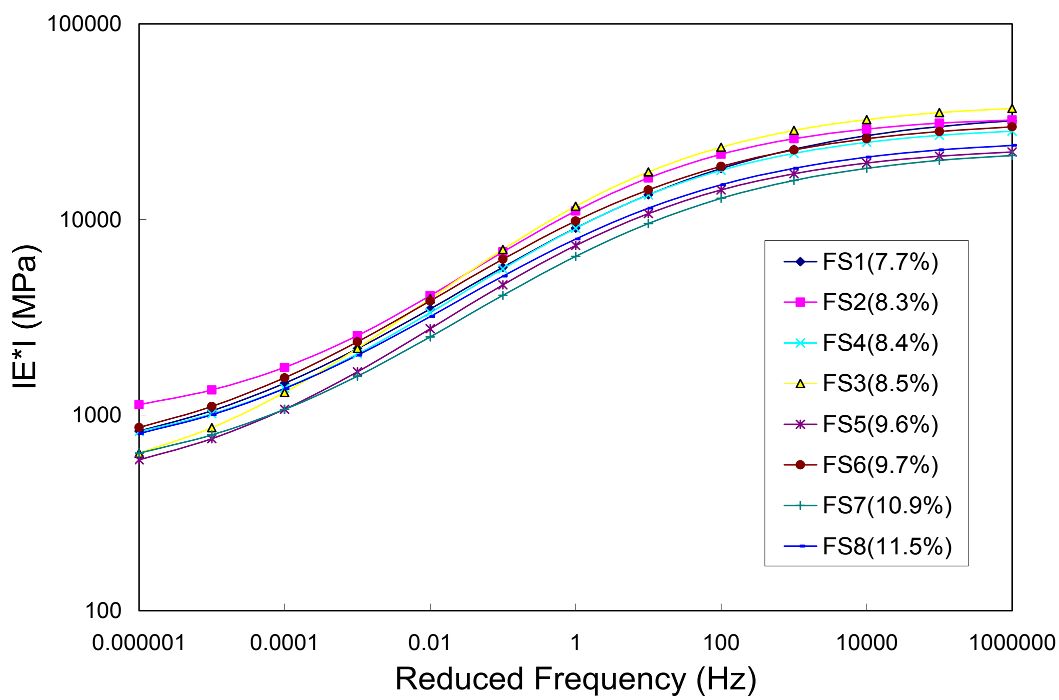

Figure 8. Effect of Air Void Content on |E*| (I19C)

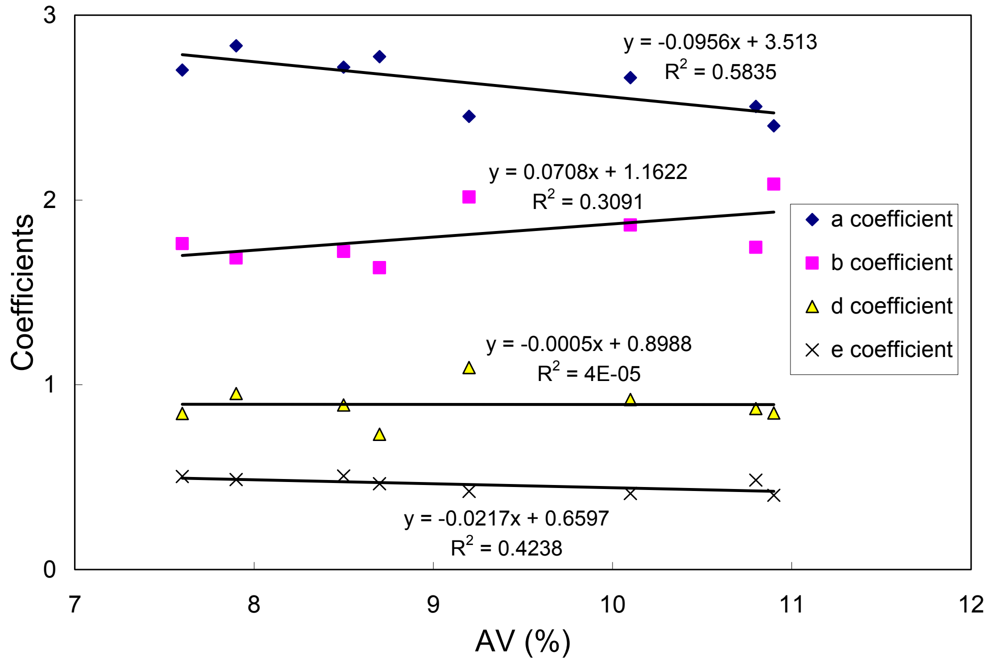

Figure 9. ∣E*∣ Coefficients vs. Air Void Content (S9.5C)

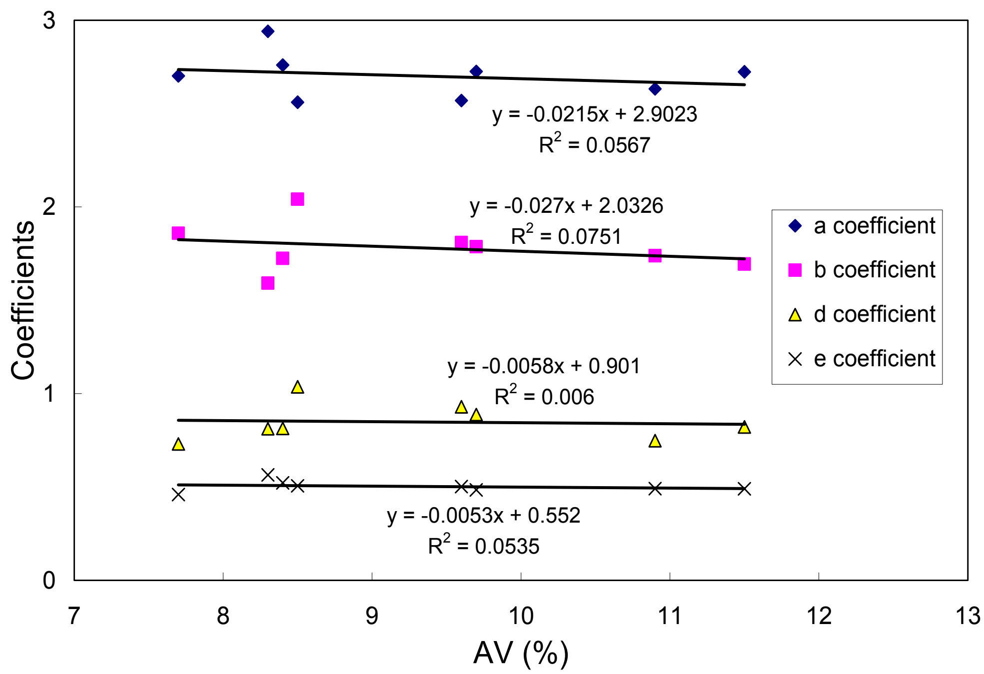

Figure 10. ∣E*∣ Coefficients vs. Air Void Content (I19C)

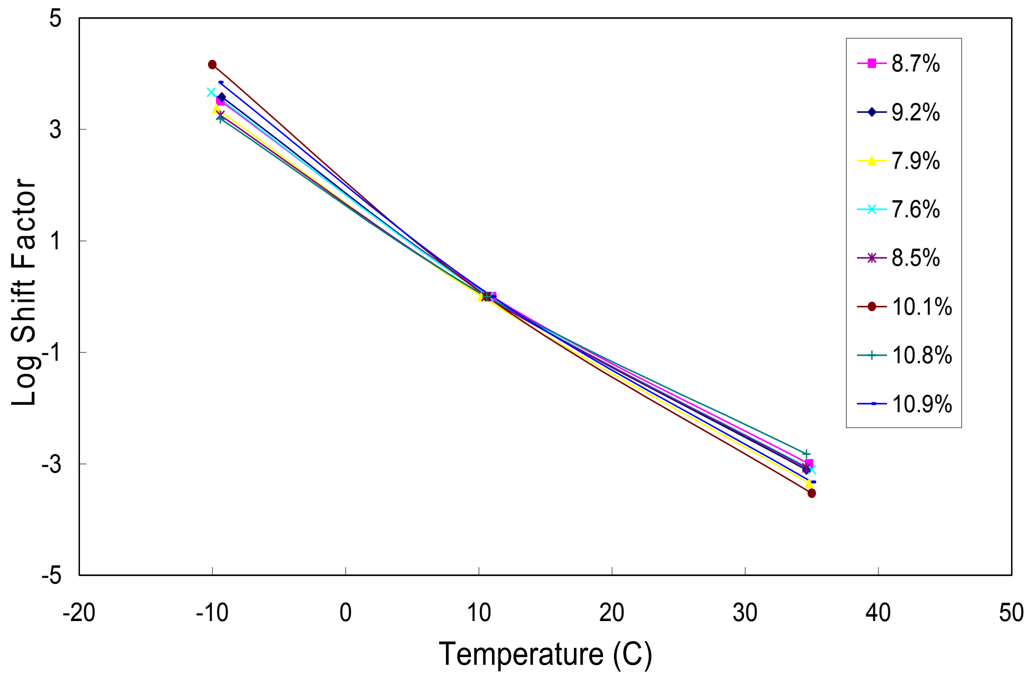

Figure 11. Shift Factor vs. Temperature (S9.5C)

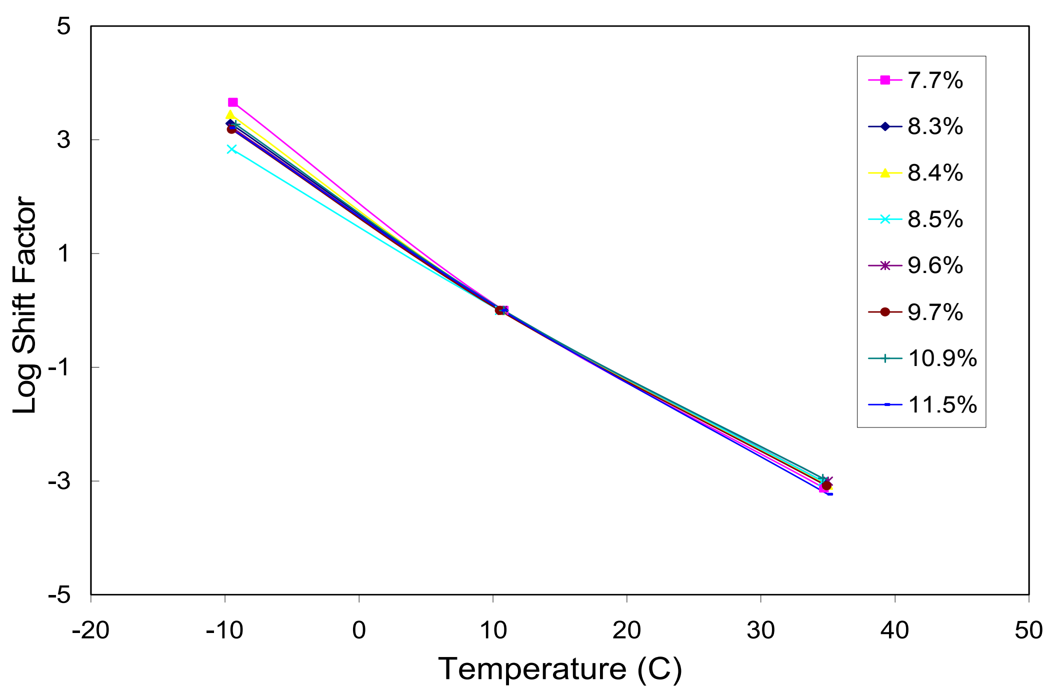

Figure 12. Shift Factor vs. Temperature (I19C)

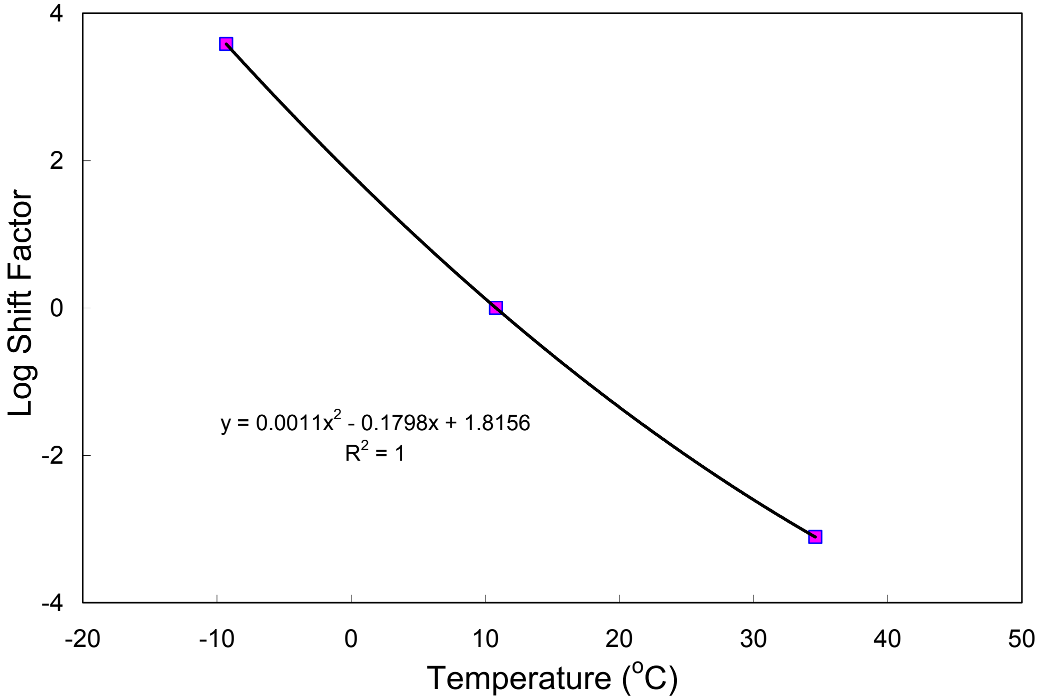

Figure 13. Best Fit Between Shift Factor and Temperature (S9.5C)

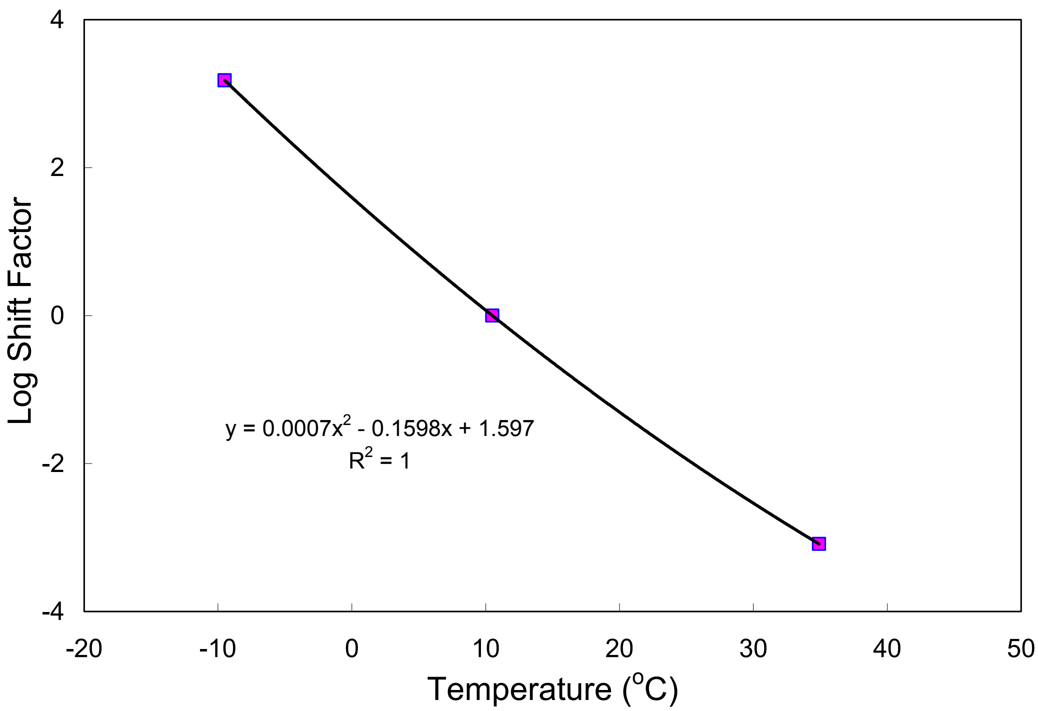

Figure 14. Best Fit Between Shift Factor and Temperature (I19C)

4.2 Triaxial Compression Testing

4.2.1 Permanent Strain Data

Triaxial compression testing data was obtained for both S9.5C and I19C mixes at 30°, 40°, and 50°C. The strain values for each test were normalized by first obtaining both the reference |E*| and the actual |E*|, as explained in the previous section. Then, the ratio between the actual and the reference |E*| was calculated and then multiplied by the strain values to get the normalized strain. If the tested specimen is soft, then the actual |E*| will be lower than the reference |E*|, and the ratio will be less than one. Multiplying this ratio by the strain will reduce the strain values. On the other hand, if the tested specimen is stiff, then the actual |E*| will be higher than the reference |E*|, and the ratio will be more than one. In this case, multiplying the ratio by the strain will increase the strain values. All the normalized triaxial compression data for the two mixes is shown in Figures 15 to 20. It is noticed by comparing the plots that the strain increases as temperature increases. Also, by looking at each graph individually it can be observed that the permanent deformation increases with the air voids. This can be more clearly demonstrated in Figures 21 and 22 at which the strain after 50,000 cycles was calculated for each test and then plotted against air voids and temperature. It is clearly shown in these two figures that the permanent strain increases as air voids and temperature increase.

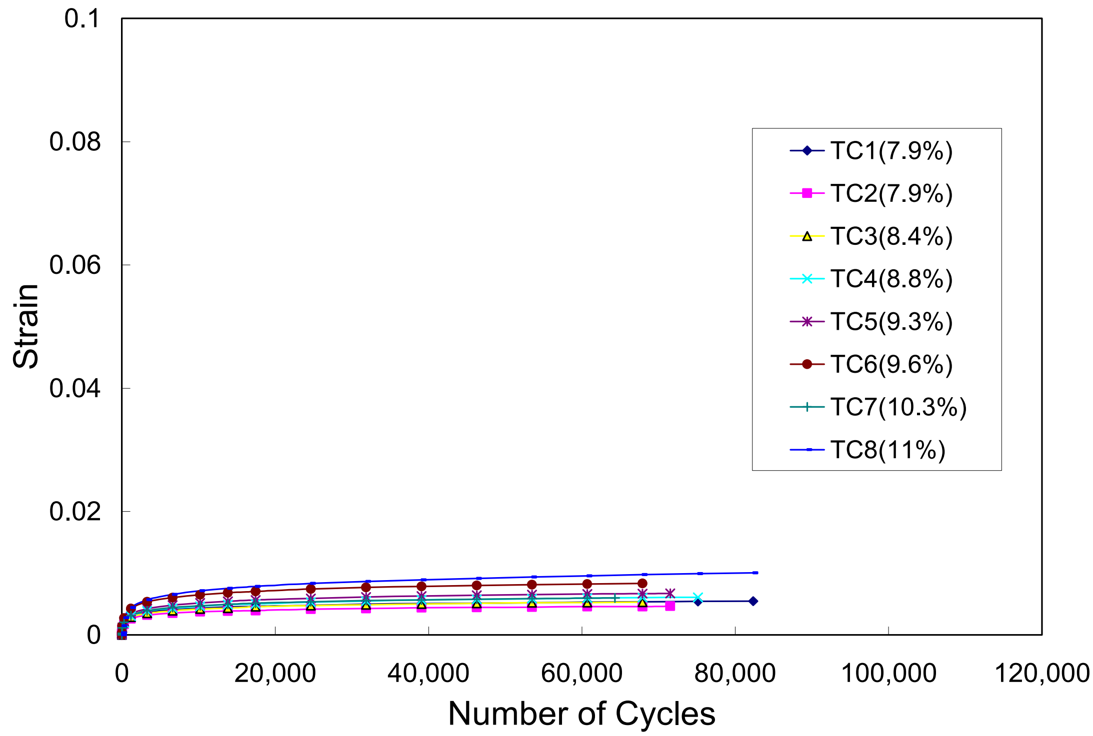

Figure 15. Triaxial Compression Testing at 30°C (S9.5C)

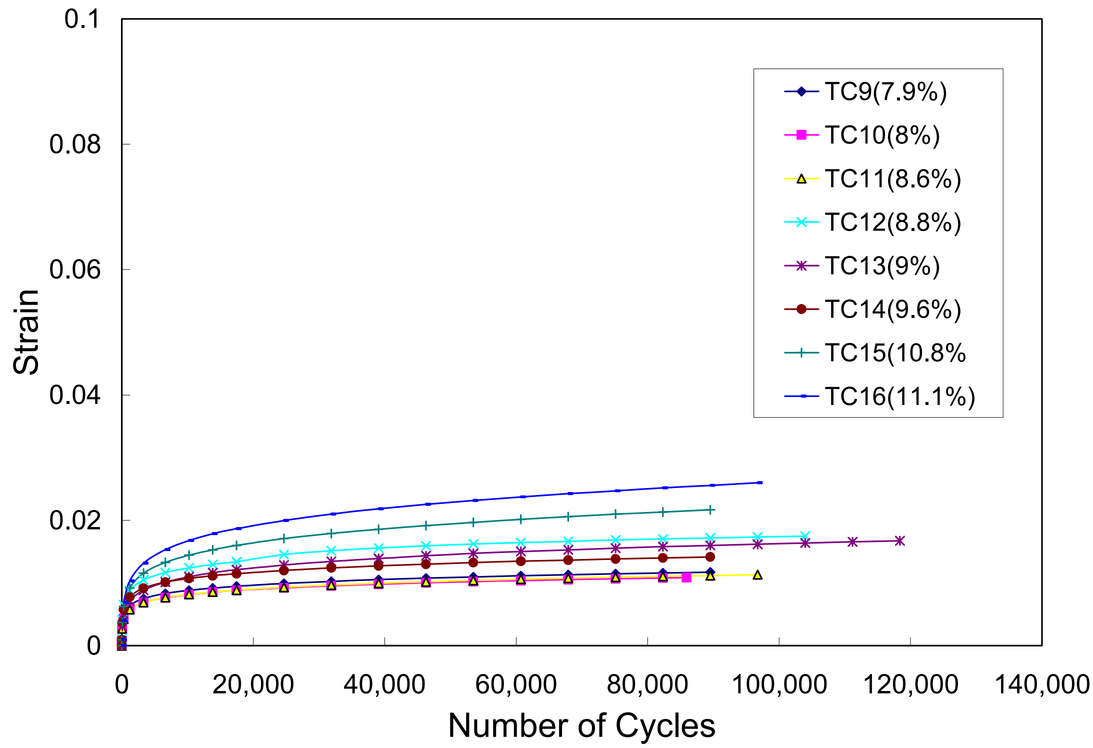

Figure 16. Triaxial Compression Testing at 40°C (S9.5C)

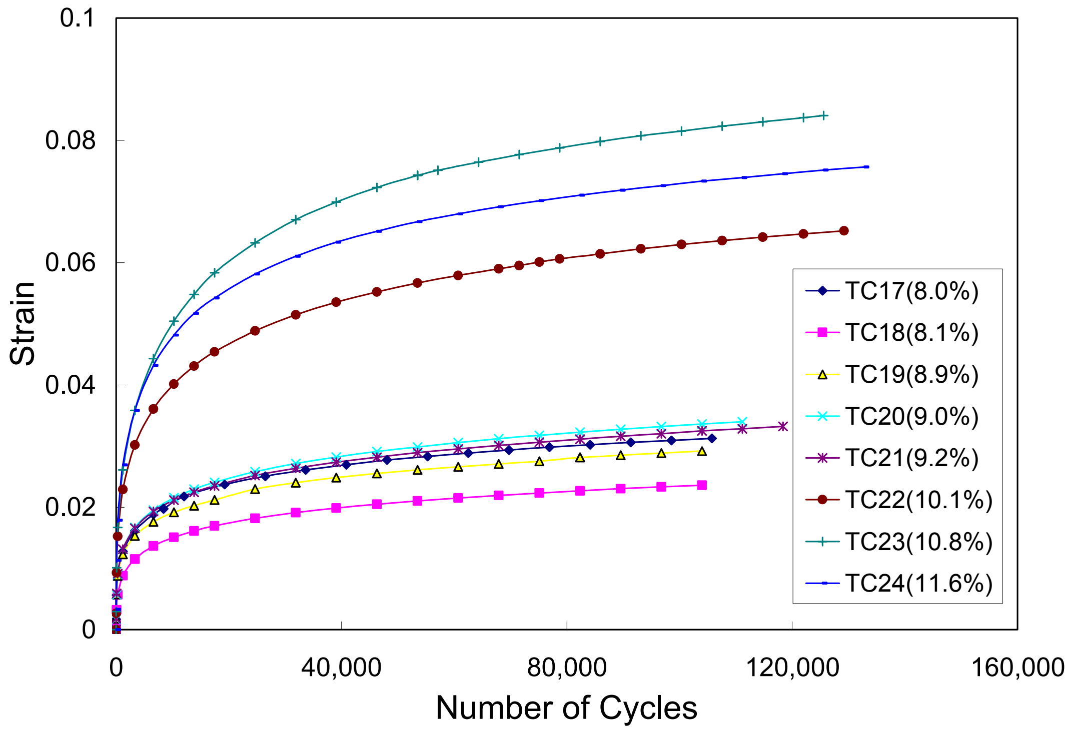

Figure 17. Triaxial Compression Testing at 50°C (S9.5C)

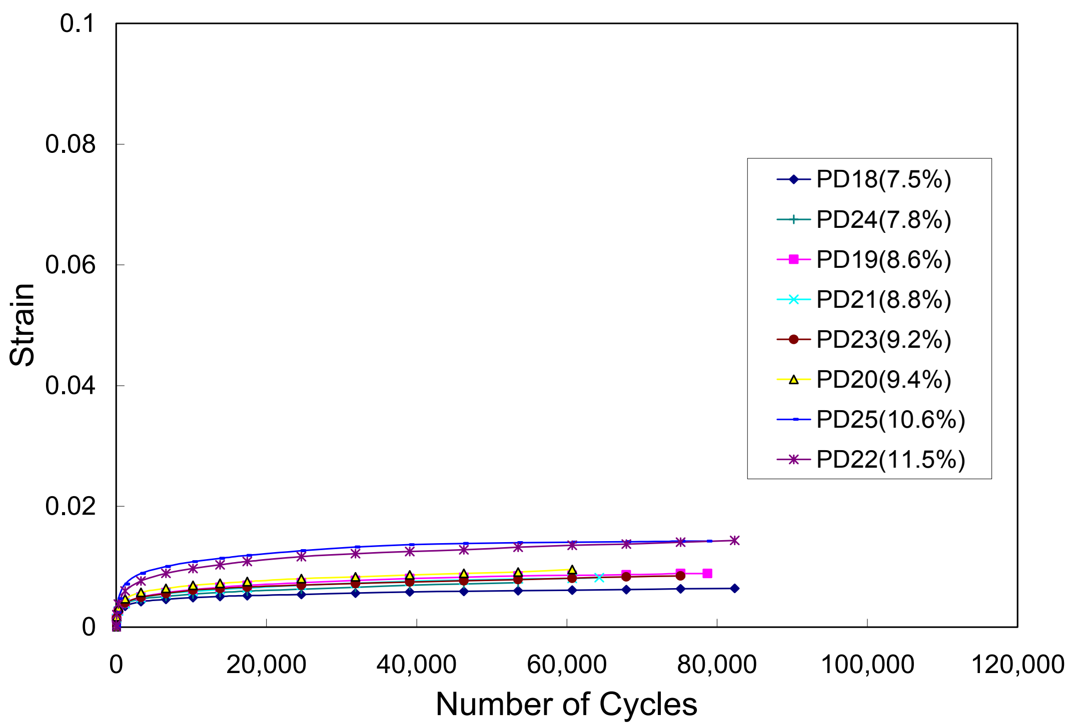

Figure 18. Triaxial Compression Testing at 30°C (I19C)

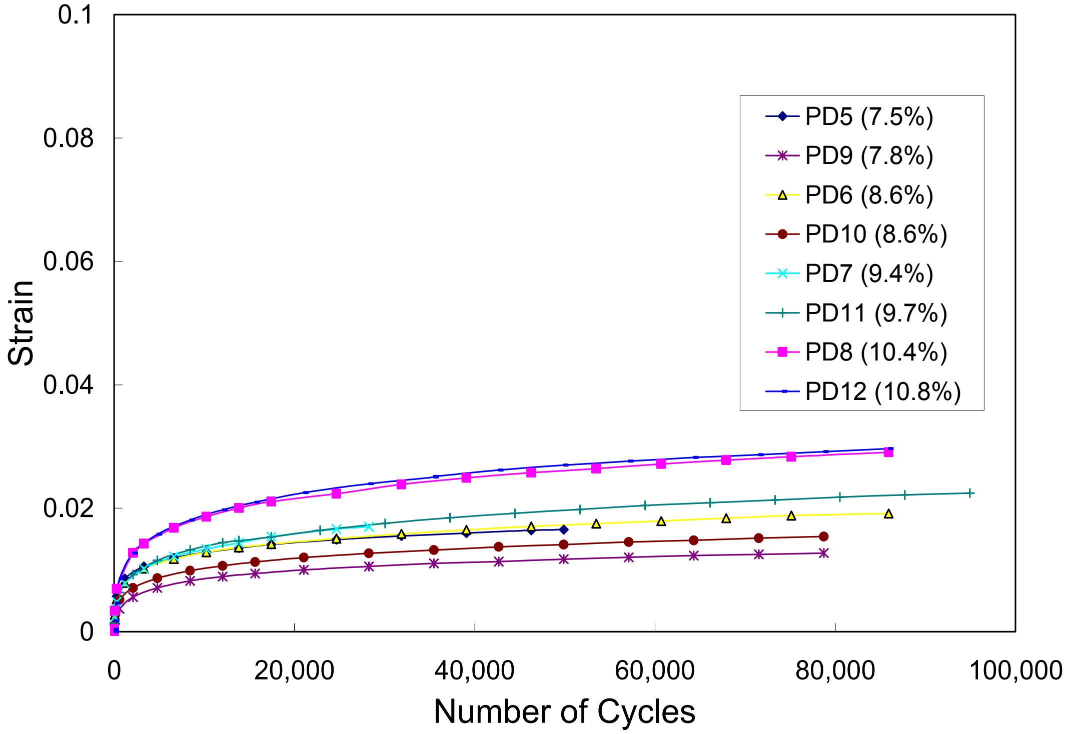

Figure 19. Triaxial Compression Testing at 40°C (I19C)

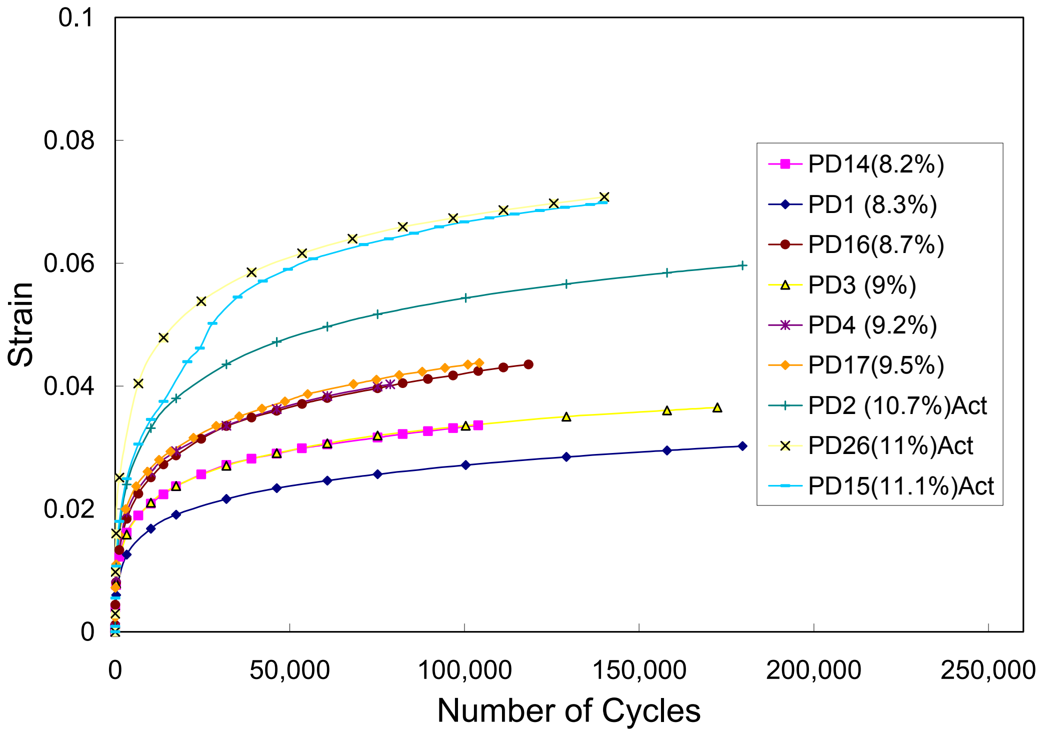

Figure 20. Triaxial Compression Testing at 50°C (I19C)

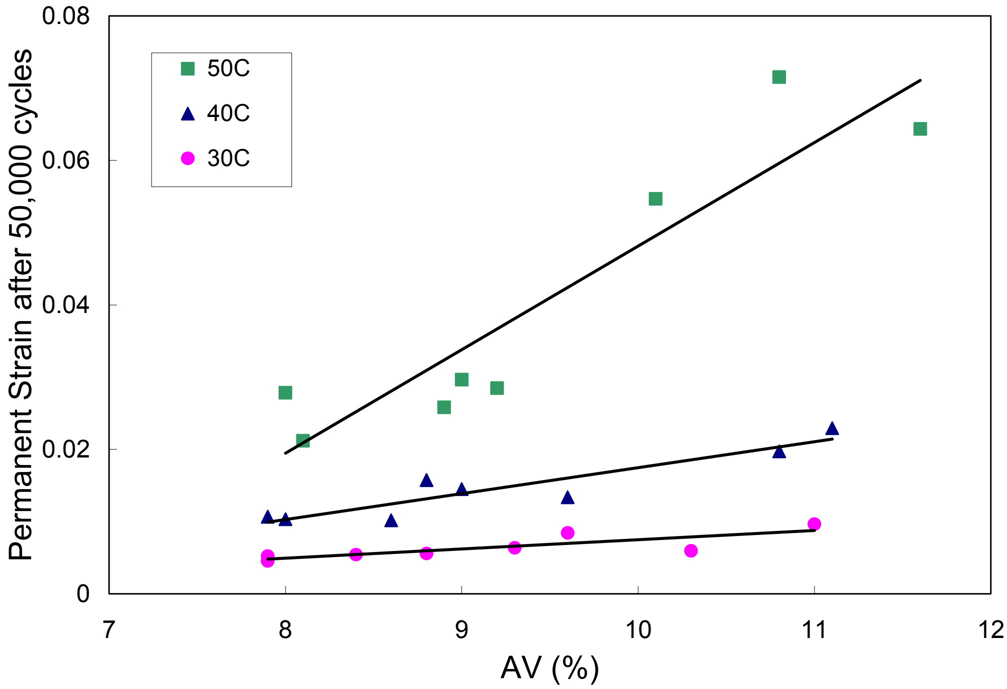

Figure 21. Permanent Strain at 50,000 cycles (S9.5C)

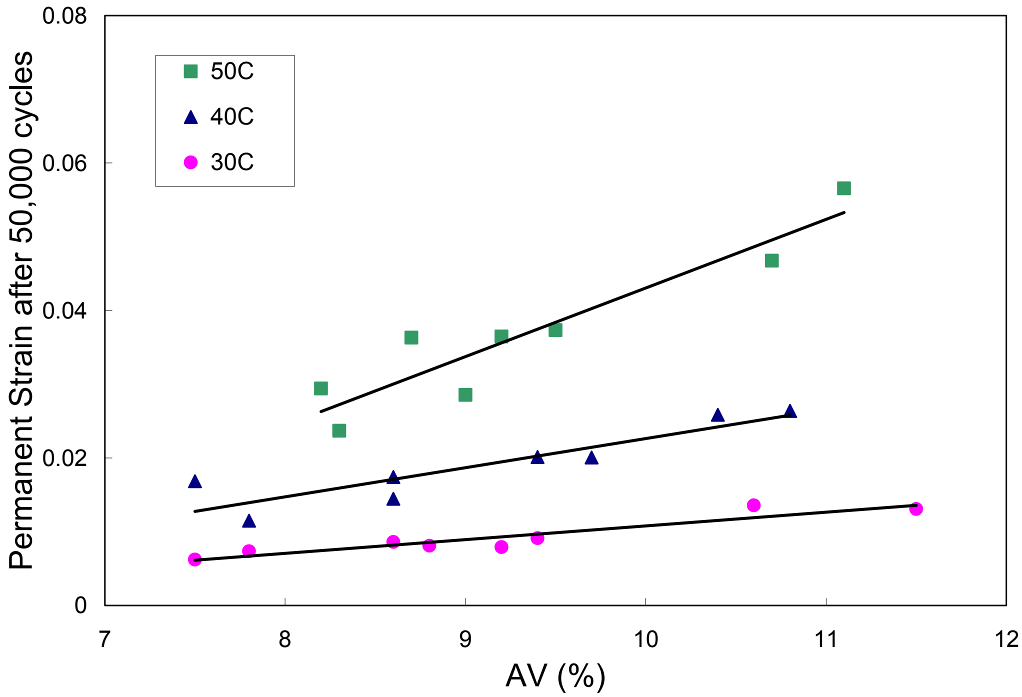

Figure 22. Permanent Strain at 50,000 cycles (I19C)

4.2.2 Regression Constants

The log-log relationship between the permanent strain and the number of load cycles is expressed by the classical power model:

$$\varepsilon_p = aN^b \qquad (11)$$

where “a” and “b” are regression constants depending upon the material-test combination conditions. The intercept “a” represents the permanent strain at N = 1. The slope “b” represents the rate of change in permanent strain as a function of the change in loading cycles (log (N)). Both “a” and “b” were obtained from each permanent deformation test. Then all the values of “a” and “b” were plotted versus air voids and temperature (Figures 23 to 26). Since the strain increases with air voids and temperature, both “a” and “b” increase with air voids and temperature, as illustrated in the figures.

SAS program was used to develop an equation for “a” and “b” coefficients as a function of both air voids (AV) and temperature (T). This relationship allows the determination of the permanent strain for any desired air voids and temperature of the asphalt concrete pavement. An examination of the trends between the plastic strain and the two independent variables (i.e., air voids and temperature) resulted in the observation that the permanent strain changes in a linear fashion with respect to air voids and in a nonlinear fashion with respect to temperature. Also, it can be observed in Figures 23 to 26 that the slope of the permanent strain and air voids relationship changes as a function of temperature. This observation indicates that there is an interaction between the air voids and temperature. Therefore, the AV*T term is introduced in the equation. To represent the nonlinear relationship between the permanent strain and temperature, both T and T^2 terms are introduced in the equation. The following are the equations obtained by the SAS program for the two mixes:

1. For the S9.5C mix,

$a = -0.0008490851 + 0.0000131784\ AV*T - 0.0000934428\ T + 0.0000013602\ T^2$

$b = 0.3203350683 + 0.0002823904\ AV*T - 0.0129807421\ T + 0.0001614234\ T^2$

2. For the I19C mix,

$a = 0.0036553841 + 0.0000045846\ AV*T - 0.0002113755\ T + 0.0000031389\ T^2$

$b = -0.1529731289 + 0.0002866283\ AV*T + 0.0132840242\ T - 0.0001671877\ T^2$

Where AV is the air voids in %, and T is the temperature in °C.

These regression equations are shown in Figures 23 to 26 in lines.

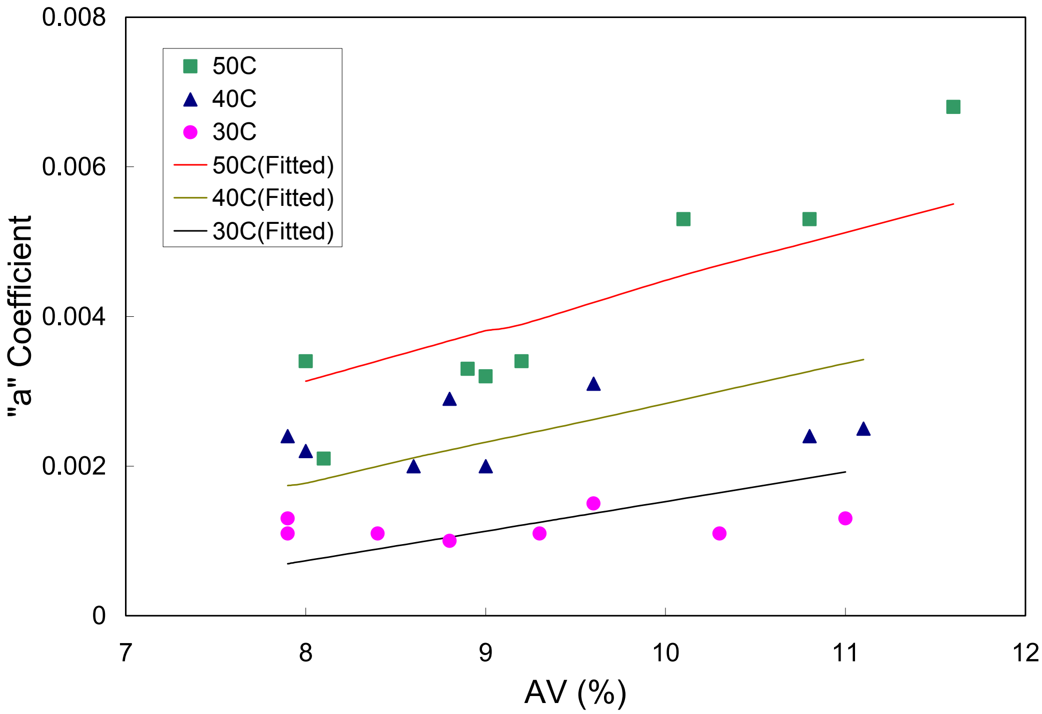

Figure 23. Effect of Air Void Content and Temperature on “a” (S9.5C)

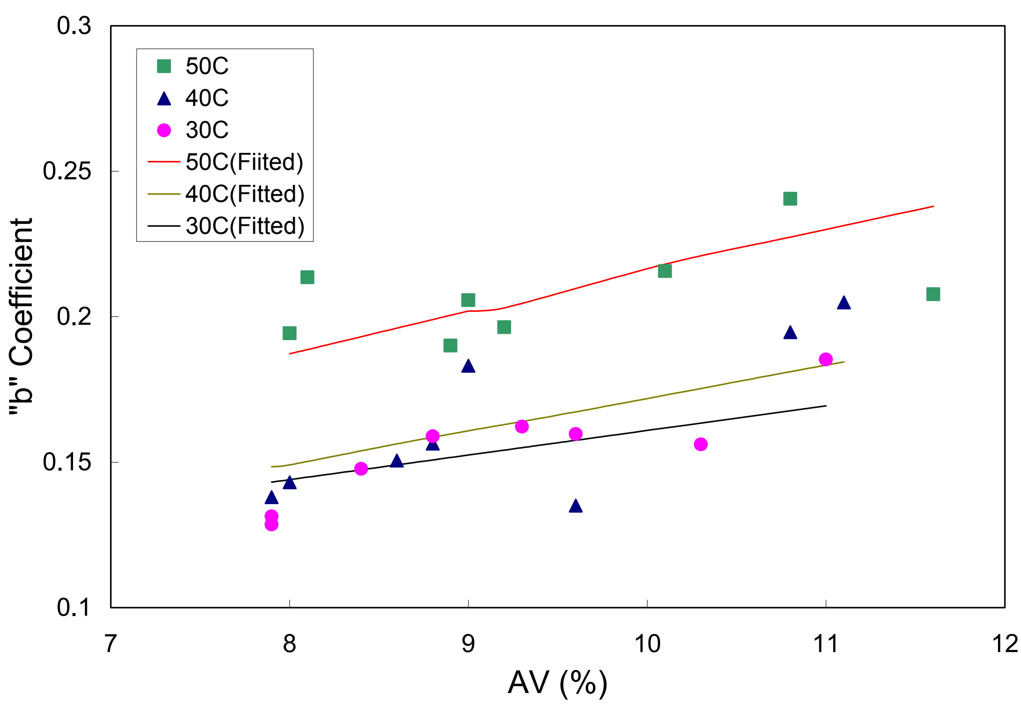

Figure 24. Effect of Air Void Content and Temperature on “b” (S9.5C)

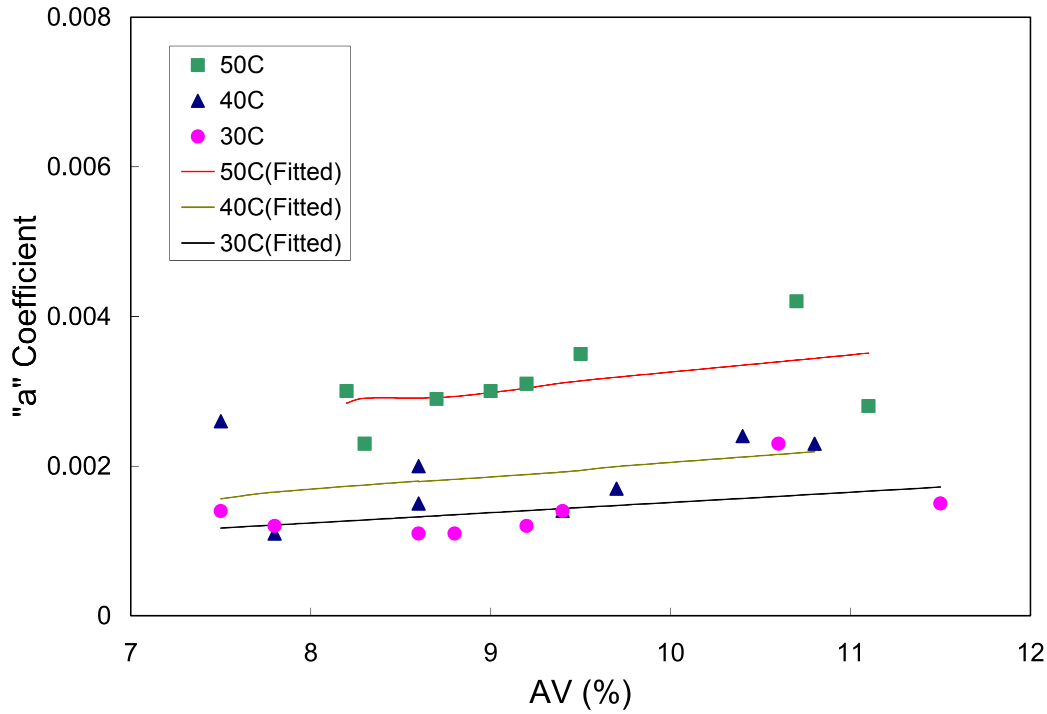

Figure 25. Effect of Air Void Content and Temperature on "a" (I19C)

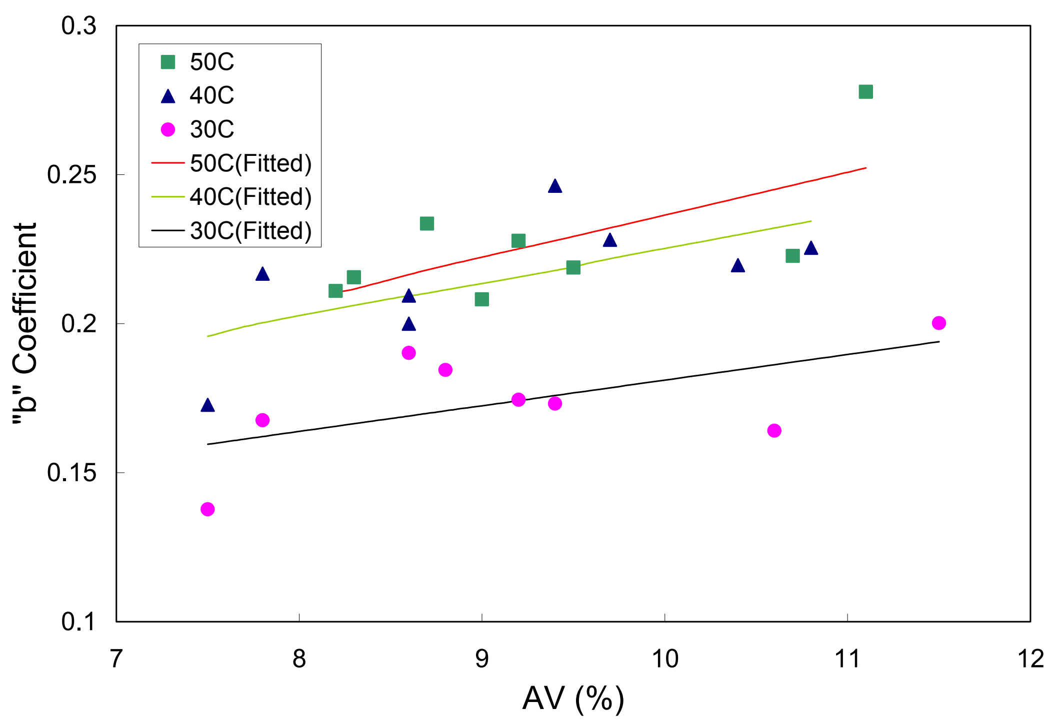

Figure 26. Effect of Air Void Content and Temperature on "b" (I19C)

4.2.3 Resilient Strain

Resilient strain is the recoverable strain resulting from the compression cycle being applied to the specimen during the triaxial compression test. The resilient strains were plotted versus number of cycles for representative tests at different temperatures as shown in Figures 27 and 28. It was found that the resilient strain in each test is relatively constant throughout the test except at the beginning of the test where the resilient strain value is low. The observation of the constant resilient strain throughout the test is important because it allows the link to be made between the permanent strain model and pavement response. This link was done in the rutting equation by dividing both sides of the equation by ε_r as shown in Eq. (12).

$$\frac{\varepsilon_{pn}}{\varepsilon_r} = (\frac{ab}{\varepsilon_r})N^{b-1} \quad (12)$$

A representative resilient strain value was obtained for each triaxial compression test by averaging the recoverable strains taken from different cycles throughout the test. The low resilient strain values that were observed in the beginning of the test were not included in this average. Then, these representative resilient strain values were plotted against air voids and temperature, as shown in Figures 29 and 30. Finally, the SAS program was used to determine an equation that relates the resilient strain to both air voids and temperature, which is shown in Figures 29 and 30 in lines. The following equations were determined for the two mixes:

1. For the S9.5C mix,

ε_r = -0.0003297399 + 0.0000002511 AV*T + 0.0000130856 T + 0.0000001867 T^2

2. For the I19C mix,

ε_r = -0.0002920861 + 0.0000008889 AV*T + 0.0000108804 T + 0.0000001122 T^2

where ε_r is the resilient strain, AV is the air voids in %, and T is the temperature in °C.

This relationship enables the user to determine the resilient strain for any asphalt pavement by inputting both air voids and temperature of the pavement.

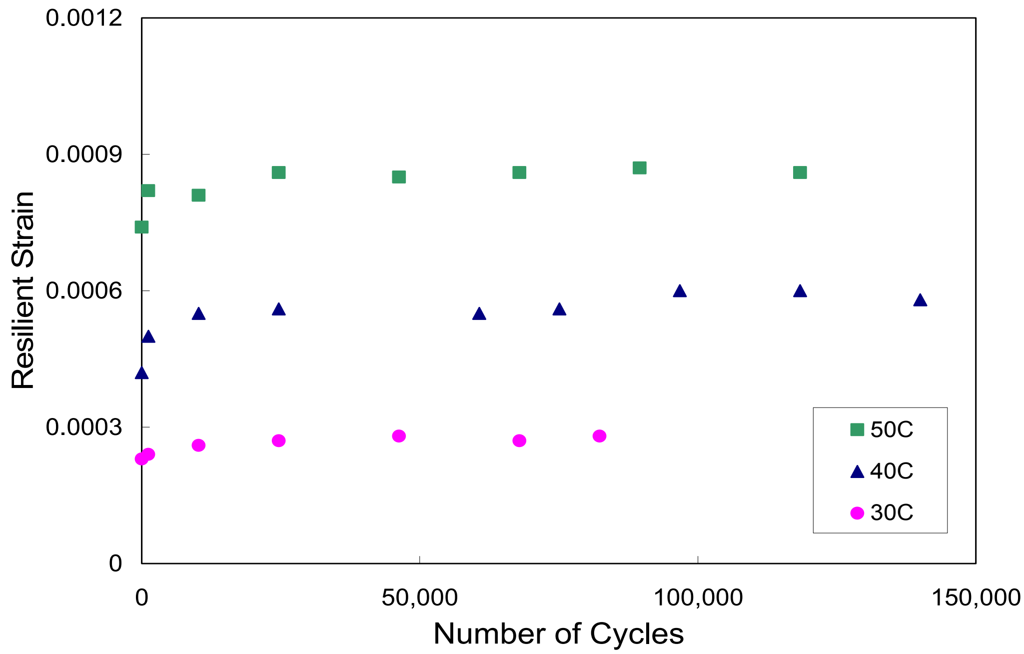

Figure 27. Resilient Strain vs. Number of Cycles for Representative Tests (S9.5C)

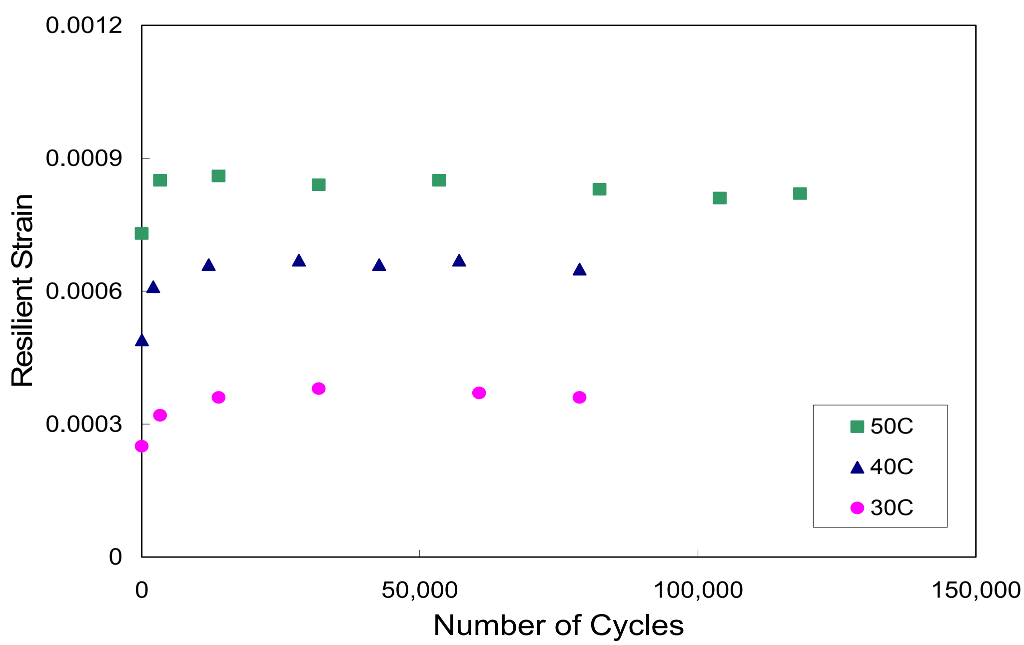

Figure 28. Resilient Strain vs. Number of Cycles for Representative Tests (I19C)

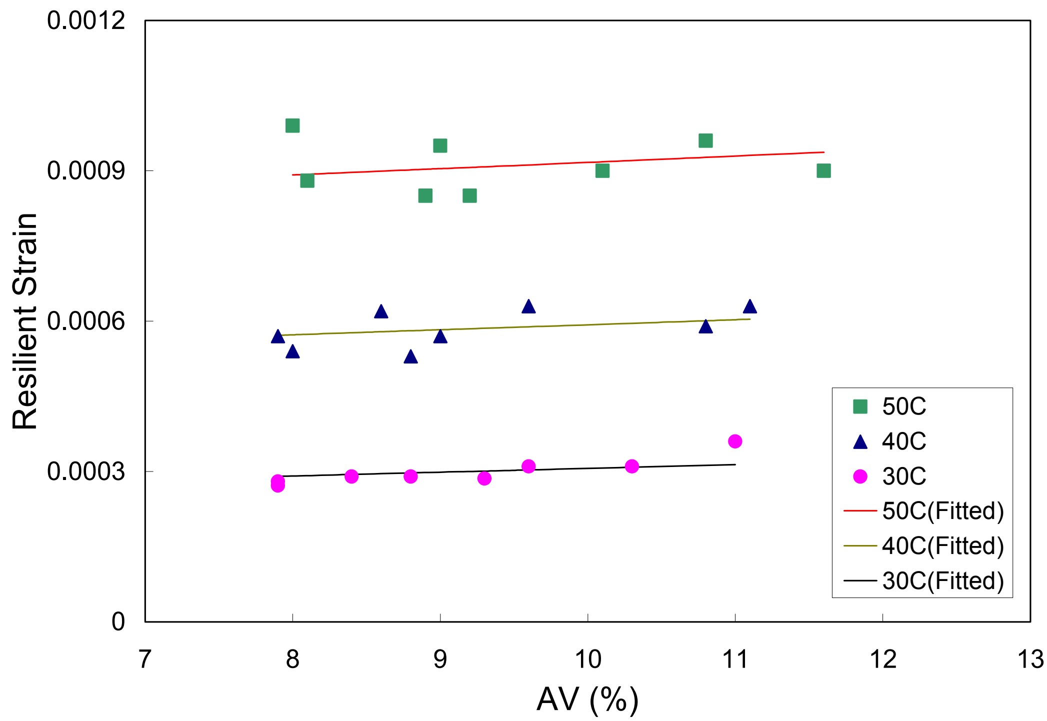

Figure 29. Effect of Air Void Content and Temperature on Resilient Strain (S9.5C)

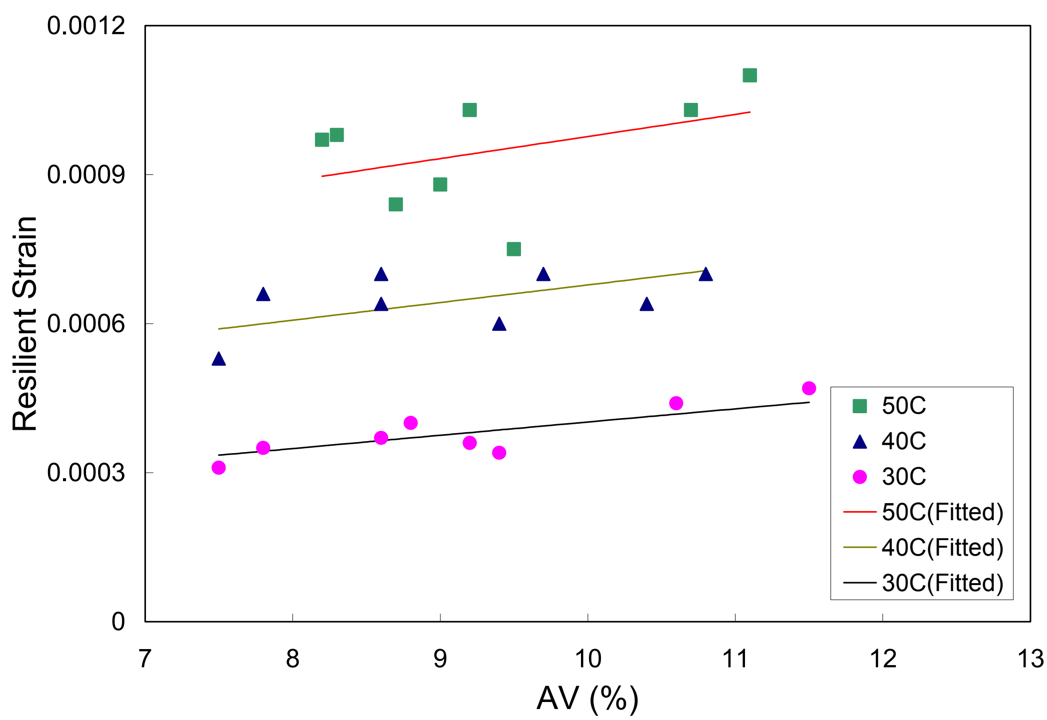

Figure 30. Effect of Air Void Content and Temperature on Resilient Strain (I19C)

4.3 Case Study

A case study was performed to see the effect of air voids on the rutting behavior of the asphalt concrete pavement. The aim of the study is to predict the yearly rut depth for a certain pavement structure once for 8% air voids and once for 11% air voids.

The pavement structure selected for this study is as follows:

- Surface course (2 inches)
- Intermediate course (4 inches)
- Crushed aggregate base (12 inches)
- Lime subgrade (semi-infinite)

The location that was selected for this study is Raleigh in North Carolina. In this analysis, the surface course was divided into two sublayers, each of 1 inch thickness, and the intermediate course was divided into three sublayers of 1, 1, and 2 inches thicknesses. This brings the total number of sublayers to five which is the maximum number of sublayers that can be evaluated by Everstress 5.0 program used in the multi layered elastic analysis. For each of the five sublayers, daily analysis was performed in order to get the rut depth for each day based on the daily traffic and the daily temperature of the sublayer. Then the rut depths were added for the 365 days to get the yearly rut depth in the sublayer. Finally, the yearly rut depths for the five sublayers were added to get the total yearly rut depth in the pavement.

First of all, the daily air temperature data for Raleigh was obtained from the National Climatic Data Center. Then, the daily air temperature was converted to pavement temperature at the middepth of each of the five sublayers using the following equation (Kim, 1994):

$$PT = (23.91 + 0.39\ D)\ \exp\ [(0.016 - 4.26\times10^{-4}D)(AT)] \qquad (13)$$

where,

PT = pavement temperature (°F),

D = depth (inches) beneath the pavement surface, and

AT = air temperature (°F).

Then, the constants a, b, and ε_r were determined for all days throughout the year from the relationships described in the previous sections in this chapter. The constants change every day based on temperature. For the top two sublayers, the coefficients of S9.5C mix were used since the top two sublayers represent the surface course of the pavement. For the bottom three sublayers, the coefficients of I19C mix were used since these sublayers represent the intermediate course mix.

Multi layered elastic analysis was performed using Everstress 5.0 program in order to determine the resilient strain for all the sublayers. Different air temperatures were selected, and for each air temperature the middepth temperature was determined for both the surface and intermediate layers using Eq. (13). Then, for each pavement temperature, dynamic modulus was determined for the two layers using Eq. (9) described in the beginning of this chapter. Then, thicknesses and moduli of the pavement layers (surface course, intermediate course, base, and subgrade) were inputted in Everstress 5.0 program and the analysis was performed to determine resilient strains for the five sublayers. The analysis was done once for each air temperature. By changing the air temperature, the pavement temperature changes, dynamic modulus changes, and the resulting resilient strains change. The whole analysis was performed twice, once for 8% and once for 11% air void content. Finally, a relationship was determined between resilient strains and air temperature for both 8% and 11% air void content. This relationship is shown in Figures 31 and 32. It can be seen from the figures that resilient strains increase with air temperature because when temperature increases, dynamic modulus decreases which results in higher resilient strains. It is also observed from the plots that the resilient strain becomes higher at the bottom sublayers. In addition, by comparing the two figures, it is noticed that resilient strains are higher for the 11% air void content than for the 8% air void content. This makes sense because the dynamic modulus is lower at the higher air voids, which results in higher resilient strains at the higher air voids. Equations between resilient strain and air temperature were developed for the five sublayers and for the two air void contents as shown in Figures 31 and 32. These equations were used in the case study to determine resilient strain for every day by knowing the air temperature of that day.

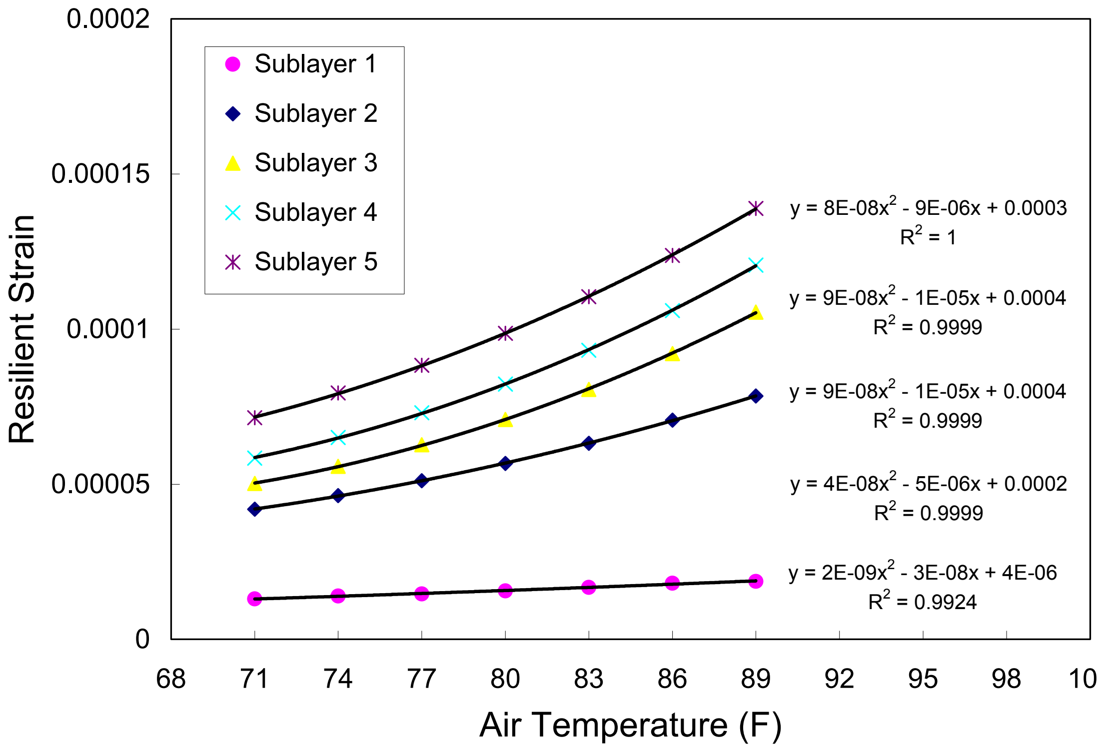

Figure 31. Resilient Strain vs. Air Temperature (for 8% Air Void Content)

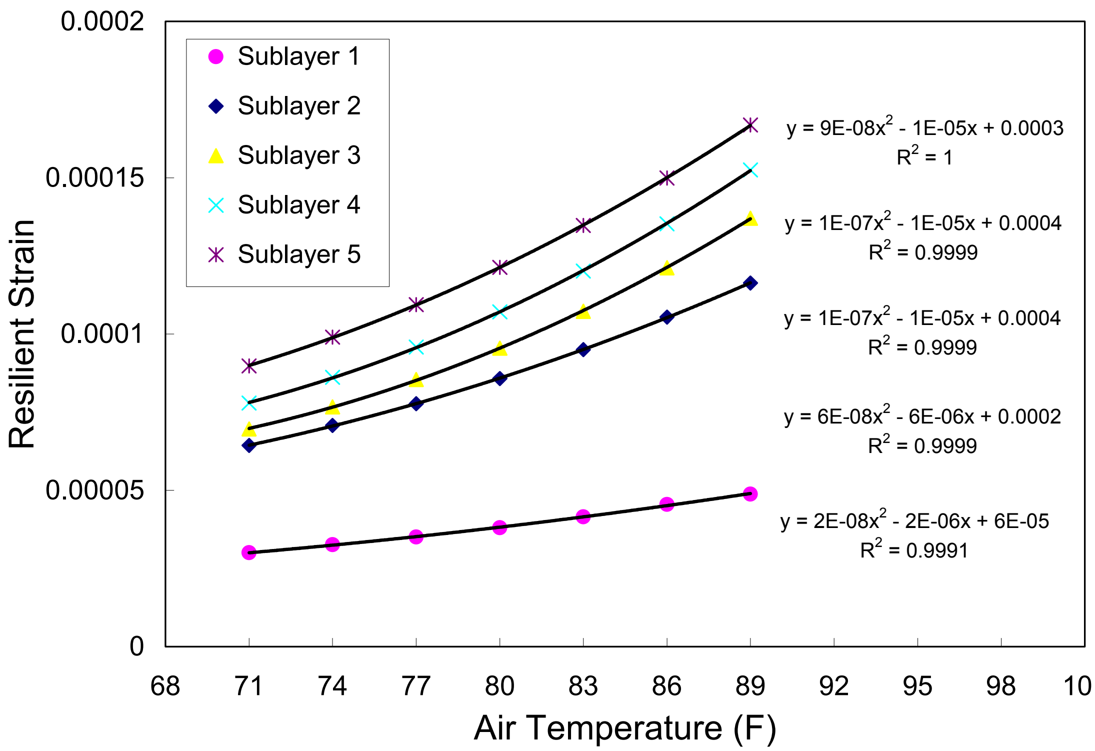

Figure 32. Resilient Strain vs. Air Temperature (for 11% Air Void Content)

In order to determine the daily rutting for the pavement, it is required to get the daily traffic of the pavement. It was assumed in this case study that the road is an urban interstate highways. The total ESALs in this case is equal to 10^7 for the pavement design life which is 20 years (Huang, 1993). The following equation was used to get the ESALs for first year:

$$\text{Total ESALs} = \sum_{N=0}^{20} T_N$$

where T_N is the traffic (in ESALs) for year N for N = 0 - 20

Since $T_N = T_\circ (1+i)^N$, then

$$\text{Total ESALs} = \sum_{N=0}^{20} T_\circ (1+i)^N$$

$$\text{Total ESALs} = T_\circ \sum_{N=0}^{20} (1+i)^N \qquad (14)$$

where,

Total ESALs (for design life) = 10^7,

T_o = ESALs for the first year,

i = growth rate = 2.5 %, and

N = years from 0 to 20.

The value of $\sum_{N=0}^{20} (1+i)^N$ was calculated to be equal to 27.18 for N = 0 to 20

Therefore,

T_o = Total ESALs / $\sum_{N=0}^{20} (1+i)^N$ = 10^7 / 27.18 = 367,918 ESALs

Daily traffic = T_o / 365 = 367,918 / 365 = 1,008 ESALs

Finally, the permanent strain was determined by solving the following equation daily for the five layers:

$$\frac{\varepsilon_{pn}}{\varepsilon_r(str)} = (\frac{ab}{\varepsilon_r})N^{b-1} \tag{15}$$

where,

a, b, and ε_r are constants determined from testing,

ε_r (str) is the resilient strain determined from multi layered elastic analysis,

N is the number of cycles (ESALs), and

ε_{pn} is the permanent strain due to a single load application; i.e., at the N^{th} application.

For the first day, the permanent strain was calculated for N = 1 to 1,008 and then they were added to get the daily strain. For second day, the strain was calculated for N = 1,009 to 2,016 by adding 1,008 ESALs for the second day, and the N values kept increasing by 1,008 for every day until the end of the year. Then, the strain was added for the 365 days to get the yearly strain and then it was multiplied by the sublayer thickness to get the rut depth for the sublayer. At the end, the rut depths were added for the five sublayers to get the total yearly rut depth in the pavement. This analysis was performed twice by changing the air voids. The resulting yearly rut depth was 0.0074 inches for 8% air voids and was 0.0168 inches for 11% air voids. Therefore, the rut depth in case of 11% air voids was 2.3 times more than the rut depth in case of 8% air voids. This means that the 11% air voids pavement will reach failure first, and therefore, it will have less service life than the in-specification pavement with 8% air voids. Also, the fact that the amount of rutting is almost doubled in the case of the deficient pavement supports the currently used policy, which is based on 50% price reduction for 3% deficiency in air voids. However, there is a need to analyze other cases involving different pavement structures before coming up with the final conclusion regarding the price reduction for density deficient asphalt mixtures.

5. CONCLUSIONS

After conducting laboratory testing on specimens with different air void contents, and after analyzing the data and comparing the results, the following conclusions can be drawn:

1. From frequency sweep testing results, it was found that the shift factor changes as a function of temperature. No trend was observed between shift factor and air void content.
2. A relationship was developed between the coefficients of the sigmoidal function and the air void content.
3. The sigmoidal function enables the user to calculate dynamic modulus for any pavement by knowing both the temperature and the air void content of the pavement.
4. Dynamic modulus decreases with the increase of both temperature and air void content as the asphalt mixture becomes softer at higher temperatures and air voids.
5. From the triaxial compression permanent deformation testing results, the regression constants were determined and related to both temperature and air void content.
6. The permanent strain increases with the increase of both temperature and air void content.
7. Resilient strain is constant throughout the permanent deformation test.

8. Resilient strain measured from the permanent deformation test increases with the increase of both temperature and air void content.
9. From multi layered elastic analysis, the following observations were made:
   a. Resilient strain increases with the increase of both pavement temperature and air void content.
   b. Resilient strain becomes higher at the bottom layers.
10. The analysis of the case study showed that the yearly rut depth for the 8% air voids pavement is 0.0074 inches, while the yearly rut depth for the 11% air voids pavement is 0.0168 inches. Therefore, the pavement with 3% deficiency in air voids had an amount of rutting which is 2.3 times that of the standard air voids pavement.

REFERENCES

Brown, S. F. and Cooper, K.E. (1984) The Mechanical Properties of Bituminous Materials for Road Bases and Base Courses. *Journal of the Association of Asphalt Paving Technologists, 53*.

Cominsky, R. J. (1994) The Superpave Mix Design Manual for New Construction and Overlays. Strategic Highway Research Program (SHRP-A-407), National Research Council, Washington, DC.

Huang, Y. H. (1993) *Pavement Analysis and Design*. New Jersey: Prentice Hall.

Kaloush, K. E. (2001) *Simple Performance Test for Permanent Deformation of Asphalt Mixtures*. PhD Thesis, Arizona State University, Tempe, Arizona.

Kaloush, K. E. and Witczak, M. W. (2002) Tertiary Flow Characteristics of Asphalt Mixtures. *Journal of the Association of Asphalt Paving Technologists*.

Kenis, W. J. (1988) The Rutting Models of Vesys. *Paving and Transportation Conference, 25*, 49-66.

Kim, N. (1994) *Development of Performance Prediction Models for Asphalt Concrete Layers*. PhD Thesis, North Carolina State University, Raleigh, North Carolina.

Kim, Y. R. (2001) *Impact of Price Reductions on The Long-Term Pavement Performance of HMA Mixes in North Carolina*. Research Proposal, North Carolina State University, Raleigh, North Carolina.

National Climatic Data Center. Retrieved July 19, 2002, from: http://lwf.ncdc.noaa.gov/oa/ncdc.html

APPENDIX A

AIR VOID REDUCTION STUDY OF ASPHALT PAVEMENT

1. Literature Review

Over the past years, extensive research efforts have focused on the evaluation of the densification process in asphalt pavements and its effect on the ability of asphalt paving mixtures to meet structural requirements. These efforts yield the conclusion that in-place air void contents should be between 3 and 8% for the mixture to perform satisfactorily under traffic. If the air voids are higher than 8%, a pavement would be more susceptible to cracking and oxidation and also to the permeability of air and moisture that eventually deteriorate the pavement serviceability. Also, if the air voids go below 3%, there would be a severe shearing deformation in the pavement, i.e., plastic flow without volume change due to less room for volume expansion, especially at high temperatures.

Hanson et al. (1) showed that densification of Hot Mix Asphalt (HMA) pavements continues beyond two years after construction due to traffic combined with environmental effects. Under high temperatures, as in Virginia and Texas, air void reductions in a pavement become significant, as shown in Figure 1.

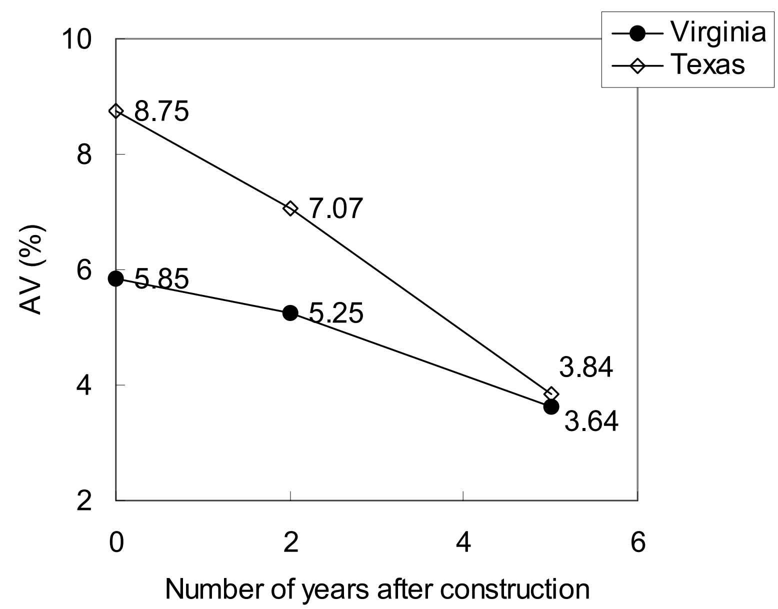

Figure 1. Change in air voids for Virginia & Texas cases

Initially, the difference in air voids between the Virginia and Texas cases was 2.9%. Then, after two years the difference reduced down to 1.82%. Finally, after five years the difference was only 0.2%. That is to say, both reached almost the same final air voids at the end of the five years despite the big difference between them at the beginning. Of course, the traffic and weather conditions may have affected these results. However, in general, this comparison suggests that pavements with high initial air voids may have a higher rate of void reduction than pavements with low initial air voids.

2. Air Void Reduction Study Using NC I-85 Data

To study the air void reduction in asphalt pavements in North Carolina, two sets of field data were collected. One set of data was obtained from the National Center for Asphalt Technology (NCAT) that is currently conducting an air void reduction study to refine the Superpave gyratory compaction requirements (2). The study includes the air void analysis of cores taken from I-85 in North Carolina immediately after construction to determine the initial air void contents and also includes the analysis of cores obtained one year later to determine air void contents after one year of traffic densification. No information on coring locations is available for this data set.

Also, the NCDOT M&T unit obtained cores from I-85 specifically for this study. In order to estimate the reduction of air void content since construction, cores were taken from between wheel paths and on the outer wheel path. Air void contents of the cores from between the wheel paths are assumed as the initial values. Air void contents of the cores from the outer wheel path are those after two years of traffic densification. Both the NCAT data (1-year traffic) and the NCDOT data (2-year traffic) are summarized in Table 1. In this table, the percent air void reduction was calculated based on the following equation:

% air void reduction = change in air void content/initial air void content × 100

The data in Table 1 are plotted in Figure 2. A careful observation of the data in Table 1 and Figure 2 reveal that the *initial* air void contents for the 2-year data are about 1% lower than those for the 1-year data. It is noted that the initial air void contents for the 1-year data are measured from cores taken immediately after paving, whereas the initial air void contents for the 2-year data are the values obtained from between the wheel paths, assuming that there is no densification at the center of the lane. Assuming that the initial air void contents in the 1-year and 2-year data are the representative values, it seems that there has been about a 1% air void reduction in the lane center during the first 2-year period. Some amount of densification in the lane center is realistic considering traffic wander and densification due to the pavement's own weight at high temperatures.

To account for this discrepancy, a 1% air void was added to the *initial* air void content of the 2-year data. After this adjustment, all the data are replotted in Figure 3. As the overall trend indicates in Figure 3, a significant air void reduction develops during the first 1-year period. After that period, the densification process becomes slower. This observation is in agreement with findings from Hanson et al. (1) who reported that the mechanical properties of field cores remained constant after two years of significant densification.

Table 1. Field Data

Initial air void	I year	2 year	Difference in air void	Percent air void reduction
8.4	7.0	-	1.4	16.7
8.4	6.6	-	1.8	21.4
9.2	6.9	-	2.3	25.0
9.4	6.4	-	3.0	31.9
10.1	6.2	-	3.9	38.6
10.4	7.4	-	3.0	28.8
10.4	6.6	-	3.8	36.5
10.9	7.6	-	3.3	30.3
11.7	8.3	-	3.4	29.1
7.39*	-	5.60	1.79	24.2
7.64	-	6.27	1.37	17.9
8.78	-	7.90	0.88	10.0
8.80	-	6.46	2.34	26.6
9.22	-	6.84	2.38	25.8
10.42	-	5.95	4.47	42.9

* Initial air void contents for 2-year data are coming from the lane center after two years of service.

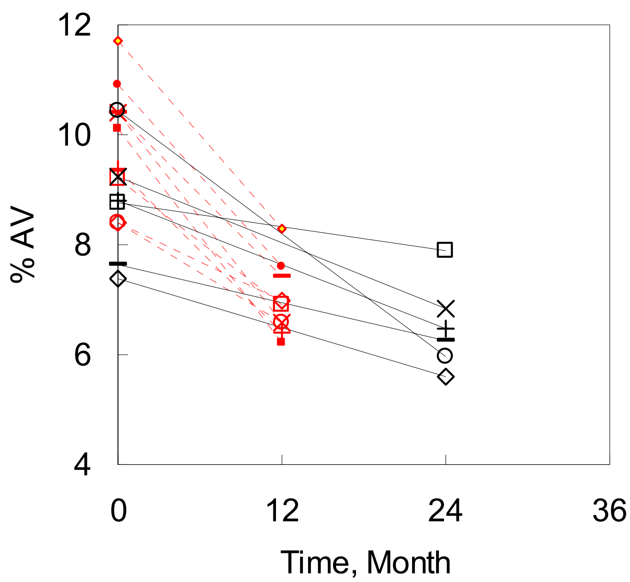

Figure 2. Reduction of Air Void Contents

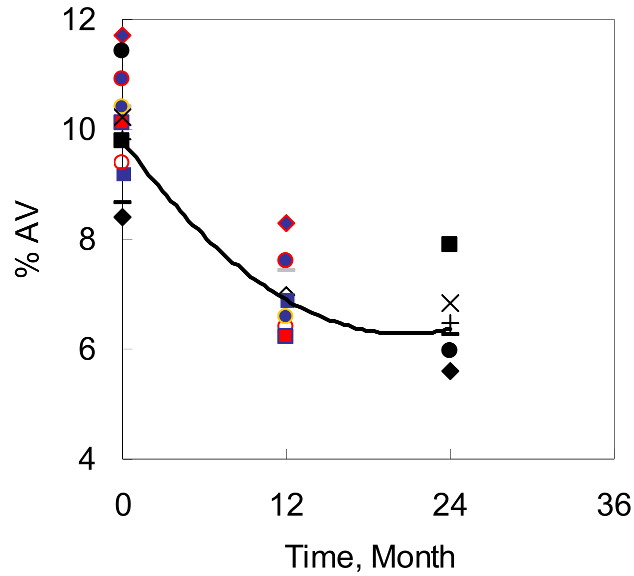

Figure 3. Percent Reduction of Air Voids after the Adjustment of the *Initial A*ir Voids

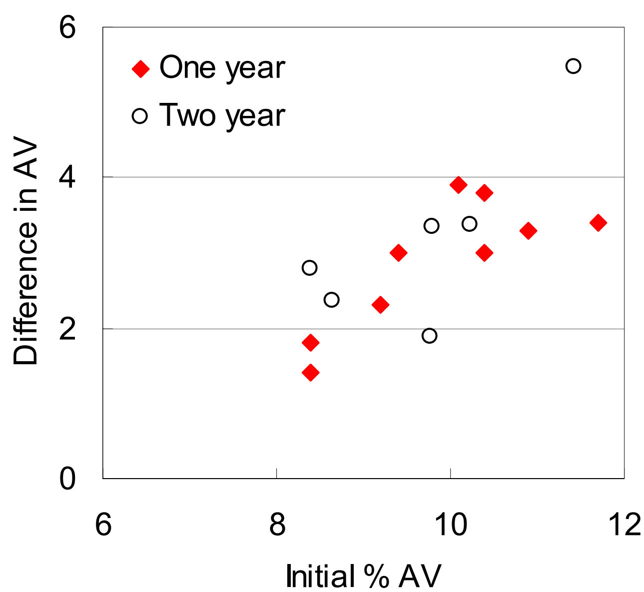

Figure 4. Difference of Air Voids

Figure 4 shows the air void difference after adjusting initial air voids of 2-year data. As mentioned previously, it is noticeable that, in general, higher initial air voids cause larger air void reductions during the densification. Field air voids investigated in this study are mostly reduced by 20 to 40% of original air voids, as presented in Figure 5.

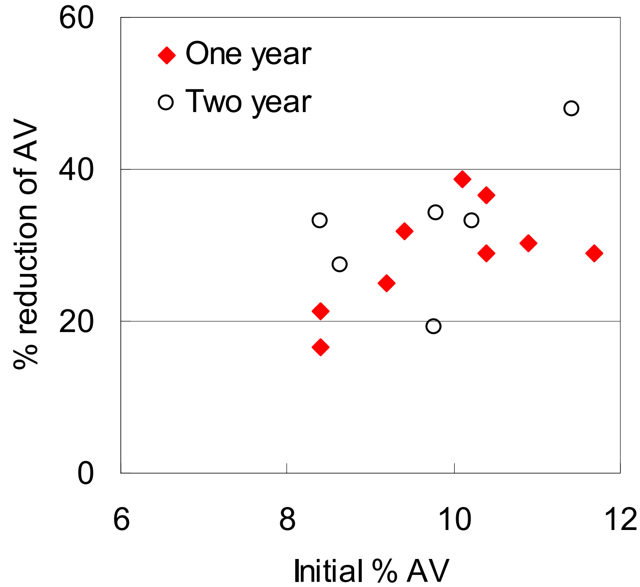

Figure 5. Percent Reduction of Air Void Contents after Two Years

3. Determination of Target Air Void Contents for Fatigue Testing

Based on the findings reported in the previous section, target air voids of specimens for fatigue testing could be selected based on final air voids as a result of two years of densification. To achieve this purpose, the air void reduction data after one year and two years are fitted to a linear function, as shown in Figure 6. As was presented in the earlier report, the density deficiency levels to be investigated in this project are 0, 0.75, 1.5, and 3% lower than the minimum 92% of maximum specific gravity specified by the NCDOT. These density values correspond to the air void contents of 8, 8.75, 9.5, and 11%. Inputting these four values to the regression equation in Figure 6 yields 6.26, 6.49, 6.71, and 7.15%. The correspondence between the initial air void contents and the laboratory target air void contents is shown in Table 2.

Since actual air void contents of fabricated specimens vary even though the target air void contents are the same, 6, 6.5, 7.0, and 7.5% are used in this study as the target air void contents for specimen fabrication purposes. Then, the fatigue life of the specimens at the four target air void contents shown in Table 2 will be determined by interpolation of the data.

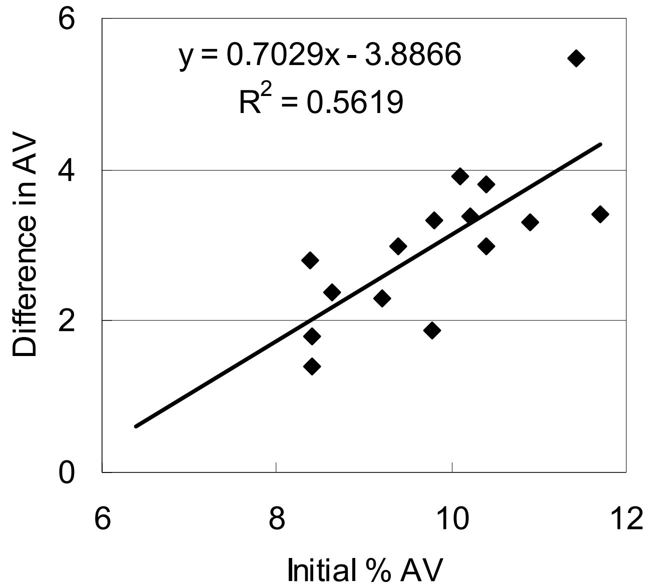

Figure 6. Air Void Reduction after Two Years (1-year NCAT Data Included)

Table 2. Initial Air Void Contents and Laboratory Target Air Void Contents

Initial air voids	Lab. target air voids
8	6.26
8.75	6.49
9.5	6.71
11.0	7.15

4. Determination of Target Air Void Contents for Permanent Deformation Testing

There are two sequential mechanisms that may affect permanent deformation in asphalt pavements (4): (a) a densification process due to the accumulation of the vertical deformation (volume change) under traffic loads; and (b) shear deformation (plastic flow) owing to the lateral deformation. Therefore, the specimens for rutting evaluation should be fabricated with the initial air voids immediately after construction since densification is part of permanent deformation.

In order to test 0, 0.75, 1.5, and 3% density deficiencies, the specimens will be fabricated with air void contents of 8, 8.75, 9.5, and 11% for the evaluation of permanent deformation.

REFERENCES

1. Hanson, D. I., R. B. Mallick, and E. R. Brown (1994). Five-Year Evaluation of HMA Properties at the AAMAS Test Projects. *Transportation Research Record, 1454*, 134-143.
2. National Center for Asphalt Technology (2002). Verification of the Gyrations in the N_{design} Table for North Carolina #1: I-85, NCHRP 9-9 (1).
3. Kaloush, K. E. and M. W. Witczak (2002). Tertiary Flow Characteristics of Asphalt Mixtures. *Journal of the Association of Asphalt Paving Technologists*.
4. E. J. Yoder and M. W. Witczak (1975). Principles of Pavement Design, 2nd Edition.

APPENDIX B

PERMANENT DEFORMATION TEST PROTOCOL

W2: Simple Performance Test for Permanent Deformation Based Upon Repeated Load Test of Asphalt Concrete Mixtures

1. Scope

1.1 This test method covers procedures for the preparation, testing and measurement of permanent deformation of cylindrical asphalt concrete specimens in a triaxial state of compressive loading.

1.2 The procedure uses a loading cycle of 1.0 second in duration, and consisting of applying 0.1-second haversine load followed by 0.9-second rest period. Permanent axial and/or radial strains are recorded through out the test.

1.3 The test is conducted at a single effective temperature T_{eff} and design stress levels.

1.4 This standard is applicable to laboratory prepared specimens 100 mm in diameter and 150 mrn in height for mixtures with nominal maximum size aggregate less than or equal to 37.5 mm (1.5 in).

1.5 *This standard may involve hazardous material, operations, and equipment. This standard does not purport to address all safety problems associated with its use. It is the responsibility of the user of this procedure to establish appropriate safety and health practices and to determine the applicability of regulatory limitations prior to use.*

2. Referenced Documents

2.1 AASHTO Standards

TP4 Method for Preparing and Determining the Density of Hot Mix Asphalt (HMA) Specimens by Means of the SHRP Gyratory Compactor

PP2 Practice for Mixture Conditioning of Hot Mix Asphalt (HMA)

T67 Standard Practices for Load Verification of Testing Machines (cross-listed with ASTM E4)

T269 Percent Air Voids in Compacted Dense and Open Bituminous Paving Mixtures

W2: Simple Performance Test for Permanent Deformation Based Upon Repeated Load Test of Asphalt Concrete Mixtures

3. Definitions

3.1 *Permanent Deformation* - is a manifestation of two different mechanisms and is a combination of densification (volume change) and repetitive shear deformation (plastic flow with no volume change).

3.2 *Flow Number* - is defined as the number of load repetitions at which shear deformation, under constant volume, starts.

3.3 *Effective Temperature* T_{eff} - Is a single test temperature at which an amount of permanent deformation would occur equivalent to that measured by considering each season separately throughout the year

4. Summary of Method

4.1 A cylindrical sample of bituminous paving mixture is subjected to a haversine axial load. The load is applied for duration of 0.l-second with a rest period of 0.9-second. The rest period has a load equivalent to the seating load. The test can be performed either without confinement, or a confining pressure is applied to better simulate in situ stress conditions. Cumulative permanent axial and radial strains are recorded through out the test. In addition, the number of repetitions at which shear deformation, under constant volume, starts is defined as the Flow Number.

5. Significance and Use

5.1 Current Superpave volumetric mix design procedure lacks a fundamental design criterion to evaluate fundamental engineering properties of the asphalt mixture that directly affect performance. In this test, the selection of the design binder content and aggregate structure is fundamentally enhanced by the evaluation of the mix resistance to shear flow (Flow Number of Repetitions).

5.2 This fundamental engineering property can be used as a performance criteria indicator for permanent deformation resistance of the asphalt concrete mixture, or can be simply used to compare the shear resistance properties of various bituminous paving mixtures.

6. Apparatus

6.1 Load Test System - A load test system consisting of a testing machine, environmental chamber, measuring system, and specimen end fixtures.

W2: Simple Performance Test for Permanent Deformation Based Upon Repeated Load Test of Asphalt Concrete Mixtures

6.1.1 *Testing Machine* - The testing machine should be capable of applying haversine loads up to 25 kN (5.600 Ibs). An electro-hydraulic machine is recommended but not necessarily required. The loading device should be calibrated as outlined in the "Equipment Calibration" Section of the testing manual.

6.1.2 *Confining Pressure Device:* a system capable of maintaining a constant confining pressure, up to 207 kPa (30 psi), such as an air pressure intensifier or a hydraulic pump. The device shall be equipped with a pressure relief valve and a system to pressurize and depressurize the cell with gas or fluid. The device should also have a high temperature control subsystem for testing up to 60°C (140°F) within an accuracy of ± 0.5 °C (1 °F) at constant pressure.

Note 1 - It has been found that feedback control of a servovalve to control the pressure is the preferred method of control. However, manual valves or proportional valves may be adequate for some applications. The axisymmetric triaxial cells of AASHTO T292 or *T294* may be used for this purpose. Other types of triaxial cells may be permitted. In all cases, see-through cells are not recommended for use with gas confining media. Sight glass ports or reduced area windows are recommended with gas media for safety reasons. It is not required that the specimen be visible through the cell wall if specimen centering and proper instrumentation operation can be verified without a see-through pressure vessel. Certain simulations of pavement loads and extended material characterization desired for local conditions may suggest using confining pressures greater than 207 KPa. For pressures higher than 690 KPa (100 psi), fluid cells are recommended.

6.1.3 *Environmental Chamber* - A chamber for controlling the test specimen at the desired temperature is required. The environmental chamber shall be capable of controlling the temperature of the specimen over a temperature range from 25 to 60 °C (77 to 140 °F) to an accuracy of ± 0.5 °C (1 °F). The chamber shall be large enough to accommodate the test specimen and a dummy specimen with temperature sensor mounted at the center for temperature verification.

Note 2 - If the chamber does not have sufficient room for a dummy specimen, it is permissible to have a second chamber controlling the temperature of the dummy. The separate dummy chamber must be operated similar to the operation of the main test specimen chamber so that the dummy will accurately register the time required to obtain temperature equilibrium on the test specimen.

6.1.4 *Measurement System* - The system shall include a data acquisition system comprising analog to digital conversion and/or digital input for storage and analysis on a computer. The system shall be capable of measuring and recording the time history of the applied load, axial and radial deformations for the time duration required by this test method. The system shall be capable of measuring the load and resulting deformations with a resolution of 0.5 percent.

6.1.4.1 *Load* - The load shall be measured with an electronic load cell having adequate capacity for the anticipated load requirements. The load cell shall be calibrated in accordance with AASHTO T67. The load measuring transducer shall have accuracy equal to or better than 0.25 percent of full scale.

Note 3 - A 25 kN (5600 lbf) load cell has been found to be the approximate maximum capacity limit for this test method because of range versus resolution factors. It is recommended that if the selected load cell capacity is 25 kN or greater, the system should be equipped with either manual or automatic amplification selection capability so that it can be used to enhance control of the system at lower anticipated loads.

6.1.4.2 *Axial and Radial Deformations* - Axial and/or radial deformations shall be measured with displacement transducers referenced to gauge points contacting the specimen. The axial deformations shall be measured at a minimum of two locations 180° apart (in plan view); radial deformations shall be measured at a minimum of four locations aligned, in planform, on diametral, perpendicular lines which intersect at the center of the specimen.

Note 4 - Analog transducers such as linear variable differential transformers (LVDTs) having a range of ± 0.5 mm (0.02 in) and inherent nonlinearity equal to or better than ± 0.025 percent of full scale have been found adequate for this purpose. Software or firmware linearization techniques may be used to improve the inherent nonlinearity. Amplification and signal conditioning techniques may be used with the ± 0.5 mm range LVDTs to obtain resolutions down to 0.001 mm (0.00004 in) or better for small strain tests conditions. These techniques may be manual or automatic. In general, increasing the resolution by manual signal amplification will result in reduction of the overall range of the instrument by the same factor.

6.1.5 *Loading Platens* - Platens, with a diameter equal to or greater than that of the test specimen are required above and below the specimen to transfer the load from the testing machine to the specimen. Generally, these platens should be made of hardened or plated steel, or anodized high strength aluminum. Softer materials will require more frequent replacement. Materials that have linear elastic modulus properties and hardness properties lower than that of 6061-T6 aluminum shall not be used.

6.1.6 *Flexible Membrane:* for the confined tests, the specimen should be enclosed in an impermeable flexible membrane. The membrane should be sufficiently long to extend well onto the platens and when slightly stretched be of the same diameter as the specimen. Typical membrane wall thickness ranges between 0.012 and 0.0625 inches (0.305 - 1.588 mm).

6.1.7 *End Treatment* - Friction reducing end treatments shall be placed between the specimen ends and the loading platens.

Note 5 - End treatments consisting of two 0.5 mm (0.02 in) thick latex sheets separated with silicone grease have been found to be suitable friction reducing end treatments.

6.2 *Gyratory Compactor* - A gyratory compactor and associated equipment for preparing laboratory specimens in accordance with AASHTO TP4 shall be used. Field cores shall meet the requirements of paragraphs 7.4 through 7.6 of this test method and any reports on cores so tested will contain a detailed description of the location of any lift boundaries within the height of the specimen (e.g. lift order, thickness and material homogeneity).

6.3 *Saw* - A machine for sawing test specimens ends to the appropriate length is required. The saw machine shall be capable of cutting specimens to the prescribed dimensions without excessive heating or shock.

Note 6 - A diamond masonry saw greatly facilitates the preparation of test specimens with smooth, parallel ends. Both single or double-bladed diamond saws should have feed mechanisms and speed controls of sufficient precision to ensure compliance with paragraphs 7.5 and 7.6 of this method. Adequate blade stiffness is also important to control flexing of the blade during thin cuts.

6.4 *Core Drill* - A coring machine with cooling system and a diamond bit for cutting nominal 100 mm (4 in) diameter test specimens.

Note 7 - A coring machine with adjustable vertical feed and rotational speed is recommended. The variable feeds and speeds may be controlled by various methods. A vertical feed rate of approximately 0.05 mm/rev (0.002 in/rev) and a rotational speed of approximately 455 RPM has been found to be satisfactory for several of the Superpave mixtures.

7. Test Specimens

7.1 *Size* - Testing shall be performed on 100 mm (4 in) diameter by 150 mm (6 in) high test specimens cored from gyratory compacted mixtures.

7.2 *Aging* - Mixtures shall be aged in accordance with the short-term oven aging procedure in AASHTO PP2.

7.3 *Gyratory Specimens* – Prepare 165 mm (6.5 in) high specimens to the required air void content in accordance with AASHTO TP-4.
In this project, gyratory specimens were prepared to 178 mm (7 in) height

7.4 *Coring* - Core the nominal 100 mm (4 in) diameter test specimens from the center of the gyratory specimens. Both the core drill and the gyratory specimen should be adequately supported to ensure that the resulting test specimen is cylindrical with sides that are smooth, parallel, and free from steps, ridges, and grooves.

7.5 *Diameter* - Measure the diameter of the test specimen at the mid height and third points along axes that are 90 degrees apart. Record each of the six measurements to the nearest 1 mm (0.05 in). Calculate the average and the standard deviation of the six measurements. If the standard deviation is greater than 2.5 mm (0.01 in) discard the specimen. For acceptable specimens, the average diameter, reported to the nearest 1 mm, shall be used in the stress calculations.

7.6 *End Preparation* - The ends of all test specimens shall be smooth and perpendicular to the axis of the specimen. Prepare the ends of the specimen by sawing with a single or double bladed saw. To ensure that the sawed samples have parallel ends, the prepared specimen ends shall meet the tolerances described below. Reject test specimens not meeting these tolerances.

7.6.1 The specimen ends shall have a cut surface waviness height within a tolerance of ± 0.05 mm across any diameter. This requirement shall be checked in a minimum of three positions at approximately 120° intervals using a straight edge and feeler gauges approximately 8-12.5 mm (0.315-0.5 in) wide or an optical comparator.

7.6.2 The specimen end shall not depart from perpendicular to the axis of the specimen by more than 0.5 degrees (i.e. 0.87 mm or 0.03 in across the diameter of a 100 mm diameter specimen). This requirement shall be checked on each specimen using a machinists square and feeler gauges.

7.7 *Air Void Content* - Determine the air void content of the final test specimen in accordance with AASHTO T269. Reject specimens with air voids that differ by more than 0.5 percent from the target air voids.

7.8 *Replicates* - The number of test specimens required depends on the number of axial and/or radial strain measurements made per specimen and the desired accuracy of the average flow time values. Table 1 summarizes the LVDTs and replicate number of specimens needed to obtain a desired accuracy limit.

Table 1. Recommended Number of Specimens

LVDTs per Specimen (Total for either vertical or horizontal, not combined total)	Number of Specimens	Estimated Standard Error of the Mean, % Per Mixture's Nominal Aggregate Size		
		12.5 mm	19 mm	37.5 mm
2	2	7.6	9.5	18.8
2	3	6.2	7.7	15.3
3	2	6.7	8.9	17.4
3	3	5.5	7.3	14.2
4	2	6.2	8.6	16.6
4	3	5.0	7.0	13.6

7.9 *Sample Storage* - Wrap completed specimens in polyethylene and store in an environmentally protected storage area at temperatures between 5 and 25°C (40 and 75°F).

Note 8 - To eliminate effects of aging on test results, it is recommended that specimens be stored no more than two weeks prior to testing.

8. Test Specimen Instrumentation

8.1 Attach mounting studs for the axial LVDTs to the sides of the specimen with epoxy cement.

Note 9 - Quick setting epoxy such as Duro Master Mend Extra Strength Quick Set QM-50 has been found satisfactory for attaching studs. Under certain conditions when using the triaxial cell with confining pressure, the mounting studs may not require gluing to the specimen. While the surface contact area of the mounting studs is normally minimized consistent with transducer support requirements, it is generally recommended that the area of the studs be sufficiently large to bridge any open void structure features evident on the cut face of the specimen. The minimum diameter mounting stud consistent with support requirements is normally set at 8 mm (0.315 in), maximum diameters have not been established. A circular stud contact surface shape is not required, rectangular or other shapes are acceptable.

8.2 The gauge length for measuring axial deformations shall be 100 mm ± 1 rnrn. Suitable alignment and spacing fixture shall be used to facilitate mounting of the axial deformation measuring hardware. The gauge length is normally measured between the stud centers.
In this project, the gauge length for measuring axial deformations was adjusted to be 75 mm in order to measure higher strains from the same displacement of LVDTs.

9. Procedure

9.1 The recommended test protocol for the Simple Performance Test for use in the Superpave volumetric mix design consists of testing the asphalt mix at one effective pavement temperature T_{eff} and one design stress level selected by the design engineer. The effective pavement temperature T_{eff} covers approximately the temperature range of 25 to 60°C (77 to 140°F). The design stress levels covers the range between 69 and 207 kPa (10-30 psi) for the unconfined tests, and 483 to 966 kPa (70-140 psi) for the confined tests. Typical confinement levels range between 35 and 207 kPa (5-30 psi).
In this project, testing temperatures are 30, 40, and 50°C. The design stress level is 120 psi, and the confining stress is 20 psi.

9.2 Place the test specimen in the environmental chamber and allow it to equilibrate to the specified testing temperature. For the confined 1ests in a standard geotechnical cell, glue the gauge points to the specimen surface as necessary, fit the flexible membrane over the specimen and mount the axial hardware fixtures to the gauge points through the membrane. Place the test specimen with the flexible membrane on in the environmental chamber. A dummy specimen with a temperature sensor mounted at the center can be monitored to determine when the specimen reaches the specified test temperature. In the absence of the dummy specimen, Table 2 provides a summary of the minimum required temperature equilibrium times for samples starting from room temperature (i.e. 25 °C).

Table 2. Recommended Equilibrium Times

Specimen Test Temperature, °C (°F)	Time, hrs
25 (77)	0.5
30 (86)	1.0
37.8 (100)	1.5
? 54.4 (130)	2.0

Unconfined Tests

9.3 After temperature equilibrium is reached, place one of the friction reducing end treatments on top of the platen at the bottom of the loading frame. Place the specimen on top of the lower end treatment, and mount the axial LVDTs to the hardware previously attached to the specimen. Adjust the LVDT to near the end of its linear range to allow the full range to be available for the accumulation of compressive permanent deformation.

9.4 Place the upper friction reducing end treatment and platen on top of the specimen. Center the specimen with the load actuator visually in order to avoid eccentric loading.

9.5 Apply a contact load equal to 5 percent of the total load that will be applied to the specimen, while ensuring the proper response of the LVDTs (i.e., check for proper direction sensing for all LVDTs).

9.6 Place the radial LVDTs in contact with the specimen, adjust the LVDTs to near the end of their linear range to allow the full range to be available for the accumulation of radial permanent deformation. Adjust and balance the electronic measuring system as necessary.

9.7 Close the environmental chamber and allow sufficient time (normally 10 to 15 minutes) for the temperature to stabilize within the specimen and the chamber.

W2: Simple Performance Test for Permanent Deformation Based Upon Repeated Load Test of Asphalt Concrete Mixtures

9.8 After the time required for the sample to reach the testing temperature, apply the haversine load which yields the desired stress on the specimen. The maximum applied load (Pmax) is the maximum total load applied to the sample, including the contact and cyclic load: Pmax = Pcontact + Pcyclic

9.9 The contact load (Pcontact) is the vertical load placed on the specimen to maintain a positive contact between loading strip and the specimen: Pcontact = 0.05 x Pmax

9.10 The cyclic load (Pcyclic) is the load applied to the test specimen which is used to calculate the permanent deformation parameters: Pcyclic = Pmax - Pcontact

9.11 Apply the haversine loading (Pcyclic) and continue until 10,000 cycles (2.8 hours) or until the specimen fails and results in excessive tertiary deformation to the specimen, whichever comes first. The total number of cycles or the testing time will depend on the temperature and the stress levels applied.

9.12 During the load applications, record the load applied, the axial and radial deflection measured from all LVDTs through the data acquisition system. Signal-to-noise ratio should be at least 10. All data should be collected in real time and collected/processed so as to minimize phase errors due to sequential channel sampling. In order to save storage space during data acquisition for 10,000 cycles, it is recommended to use the data acquisition of the cycles shown in Table 3.

Table 3. Suggested Data Collection for the Repeated Load Permanent Deformation Test

Data Collected During Cycles	Data Collected During Cycles	Data Collected During Cycles
1 through 100	700	4,500
130	750	5,000
170	800	5,500
200	850	6,000
230	900	6,500
270	950	7,000
300	1,000	7,500
350	1,300	8,000
400	1,700	8,500
450	2,000	9,000
500	2,300	9,500
550	2,700	10,000
600	3,000	
650	4,000	

W2: Simple Performance Test for Permanent Deformation Based Upon Repeated Load Test of Asphalt Concrete Mixtures

Confined Tests

9.13 After temperature equilibrium is reached, place one of the friction reducing end treatments on top of the platen at the bottom of the loading frame. Place the specimen on top of the lower end treatment, place the top platen and extend the flexible membrane over the top and bottom platens. Attach the O-rings to seal the specimen on top and bottom platens from the confining air/fluid. Center the specimen with the load actuator visually in order to avoid eccentric loading.

9.14 Mount the axial LVDTs to the hardware previously attached to the specimen. Adjust the LVDT to near the end of its linear range to allow the full range to be available for the accumulation of compressive permanent deformation.

9.15 Connect the appropriate hose through the upper or lower platen (or take other appropriate steps) to keep the specimen's internal void structure under atmospheric pressure while pressure greater than atmospheric is applied to the outside of the membrane during testing.

9.16 Assemble the triaxial cell over the specimen, ensure proper seal with the base and connect the fluid (or gas) pressure lines.

9.17 Apply a contact load equal to 5 percent of the load that will be applied to the specimen, while ensuring the proper response of the LVDTs (i.e., both decrease accordingly). Place the radial LVDTs in contact with the specimen, adjust the LVDTs to near the end of their linear range to allow the full range to be available for the accumulation of radial permanent deformation.

9.18 Record the initial LVDT readings and slowly increase the lateral pressure to the desired test level (e.g. 2 psi/sec), Adjust and balance the electronic measuring system as necessary. Close the environmental chamber and allow sufficient time (normally 10 to 15 minutes) for the temperature to stabilize within the specimen and the chamber.

9.19 After the time required for the sample to reach the testing temperature, apply the haversine load which yields the desired stress on the specimen. Continue until 10,000 cycles (2.8 hours) or until the specimen fails and results in excessive tertiary deformation to the specimen, whichever comes first. The total number of cycles or the testing time will depend on the temperature and the stress levels applied.

9.20 During the load applications, record the load applied, confining pressure, the axial and radial deflection measured from all LVDTs through the data acquisition system. Signal-to-noise ratio should be at least 10. All data should be collected in real time and collected/processed so as to minimize phase errors due to sequential channel sampling. In order to save storage space during data acquisition for 10,000 cycles, it is recommended to use the data acquisition of the cycles shown in Table 3.

10. Calculations

10.1 Calculate the average axial deformation for each specimen by averaging the readings from the two axial LVDTs (In this project, four axial LVDTs). Convert the average deformation values to total axial strain (ε_{Ta}), mm/mm, by dividing by the gauge length, 100 mm (In this project, 75 mm).

10.2 Compute the cumulative axial permanent strain.

10.3 Plot the cumulative axial permanent strain versus number of loading cycles in log space. Determine the permanent deformation parameters, intercept (a) and slope (b), from the linear portion of the permanent strain curve.

10.4 The flow number of repetitions is viewed as the lowest point in the curve of rate of change in axial strain vs. number of loading cycles. The rate of change of axial strain versus number of loading cycles should be plotted and the flow number (F_N) is estimated where a minimum or zero slope is observed.

11. Report

11.1 Report all specimen information including mix identification, storage conditions, dates of manufacturing and testing, specimen diameter and length, volumetric properties, stress levels used, confining pressure, axial permanent deformation parameters: a, b and flow number of repetitions.

APPENDIX C

DYNAMIC MODULUS TEST PROTOCOL

NCHRP 1-37A Draft Test Method DM-1
Standard Test Method for Dynamic Modulus of Asphalt Concrete Mixtures
ASU – June 2002

1. Scope

1.1 This test method covers procedures for preparing and testing asphalt concrete mixtures to determine the dynamic modulus and phase angle over a range of temperatures and loading frequencies.

1.2 This standard is applicable to laboratory prepared specimens of mixtures with nominal maximum size aggregate less than or equal to 37.5 mm (1.48 in).

1.3 *This standard may involve hazardous material, operations, and equipment. This standard does not purport to address all safety problems associated with its use. It is the responsibility of the user of this procedure to establish appropriate safety and health practices and to determine the applicability of regulatory limitations prior to use.*

2. Referenced Documents

2.1 AASHTO Standards

T312 Method for Preparing and Determining the Density of Hot Mix Asphalt (HMA) Specimens by Means of the Superpave Gyratory Compactor.

PP2 Practice for Mixture Conditioning of Hot Mix Asphalt (HMA).

T166 Bulk Specific Gravity of Compacted Bituminous Mixtures.

T209 Maximum Specific Gravity of Bituminous Paving Mixtures.

T269 Percent Air Voids in Compacted Dense and Open Bituminous Paving Mixtures.

3. Definitions

3.1 *Complex Modulus* – E^*, a computed value that defines the relationship between stress and strain for a linear viscoelastic material.

3.2 *Dynamic Modulus* – $|E^*|$, the absolute value of the complex modulus calculated by dividing the maximum (peak-to-peak) stress by the recoverable (peak-to-peak) axial strain for a material subjected to a sinusoidal loading.

3.3 *Phase angle* – ϕ, the angle in degrees between a sinusoidal applied (peak to peak) stress and the resulting (peak to peak) strain in a controlled-stress test.

3.4 *Linear viscoelastic* – within the context of this test, refers to behavior in which the dynamic modulus is independent of stress or strain amplitude.

4. Summary of Method

4.1 A sinusoidal (haversine) axial compressive stress is applied to a specimen of asphalt concrete at a given temperature and loading frequency. The applied stress and the resulting recoverable axial strain response of the specimen is measured and used to calculate the dynamic modulus and phase angle.

4.2 Figure 1 presents one schematic of the dynamic modulus test that is in use.

5. Significance and Use

5.1 Dynamic modulus values measured over a range of temperatures and frequencies of loading can be shifted into a master curve for characterizing asphalt concrete for pavement thickness design and performance analysis.

5.2 The values of dynamic modulus and phase angle can also be used as performance criteria for asphalt concrete mixture design.

6. Apparatus

6.1 Dynamic Modulus Test System – A dynamic modulus test system consisting of a testing machine, environmental chamber, and measuring system.

6.1.1 *Testing Machine* – A servo-hydraulic testing machine capable of producing a controlled haversine compressive loading. The testing machine should have a capability of applying load over a range of frequencies from 0.1 to 25 Hz and stress level up to 2800 kPa (400 psi).

6.1.2 *Environmental Chamber* – A chamber for controlling the test specimen at the desired temperature. The environmental chamber shall be capable of controlling the temperature of the specimen over a temperature range from -10 to 60 ^{o}C (14 to 140 ^{o}F) to an accuracy of ± 0.5 ^{o}C (1 ^{o}F). The chamber shall be large enough to accommodate the test specimen and a dummy specimen with thermocouple mounted at the center for temperature verification.

6.1.3 *Measurement System* - The system shall be fully computer controlled capable of measuring and recording the time history of the applied load, and the axial deformations. The system shall be capable of measuring the period of the applied sinusoidal load and resulting deformations with a resolution of 0.5 percent.

6.1.3.1 *Load* - The load shall be measured with an electronic load cell in contact with one of the specimen caps. The load cell shall be calibrated in accordance with AASHTO T67. The load measuring system shall have a minimum range of 0 to 25 kN (0 to 5600 lb) with a resolution of 5 N (1 lb).

6.1.3.2 *Axial Deformations* – Axial deformations shall be measured with linear variable differential transformers (LVDT) mounted between gauge points glued to the specimen as shown in Figure 2. The deformations shall be measured at a minimum of two locations 180^o apart; however, three locations located 120^o apart is recommended to minimize the number of replicate specimens required for testing. The LVDTs shall have a range of ± 0.5 mm (0.02 in). The deformation measuring system shall have auto zero and selectable ranges as defined in Table 1.

Table 1. Deformation Measuring System Requirements.

Range, mm (in)	Resolution, mm (in)
±0.5 (0.01969)	0.0100 (0.00039)
±0.25 (0.00984)	0.0050 (0.00020)
±0.125 (0.00492)	0.0025 (0.00010)
±0.0625 (0.00246)	0.0010 (0.00004)

6.1.4 *Loading Platens* – Platens, with a diameter equal to or greater than that of the test specimen are required above and below the specimen to transfer the load from the testing machine to the specimen. Generally, these platens should be made of hardened or plated steel, or anodized high strength aluminum. Softer materials will require more frequent replacement. Materials that have linear elastic modulus properties and hardness properties lower than that of 6061-T6 aluminum shall not be used.

6.1.5 *End Treatment* – Friction reducing end treatments shall be placed between the specimen ends and the loading platens. The end treatments shall consist of two 0.5 mm (0.02 in) thick latex sheets separated with silicone grease.

6.2 *Superpave Gyratory Compactor* – A gyratory compactor and associated equipment for preparing laboratory specimens in accordance with AASHTO T312.

6.3 *Saw* – A machine for sawing test specimens ends to the appropriate length is required. The saw shall have a diamond cutting edge and shall be capable of cutting specimens to the prescribed dimensions without excessive heating or shock.

> Note 1 – A diamond masonry saw greatly facilitates the preparation of test specimens with smooth, parallel ends. Both single or double-bladed diamond saws should have feed mechanisms and speed controls of sufficient precision to ensure compliance with paragraphs 9.5 and 9.6 of this method. Adequate blade stiffness is also important to control flexing of the blade during thin cuts.

6.4 *Core Drill* - A coring machine with cooling system and a diamond bit for cutting nominal 101.6 mm (4.00 in) diameter test specimens.

> Note 2 – A coring machine with adjustable vertical feed and rotational speed is recommended. The variable feeds and speeds may be controlled by various methods. A vertical feed rate of approximately 0.05 mm/rev (0.002 in/rev) and a rotational speed of approximately 450 RPM has been found to be satisfactory for several of the Superpave mixtures.

7. Hazards

Observe standard laboratory safety precautions when preparing and testing HMA specimens.

8. Testing Equipment Calibration

8.1 The testing system shall be calibrated prior to initial use and at least once a year thereafter or per manufacturer requirements.

8.1.1 Verify the capability of the environmental chamber to maintain the required temperature within the accuracy specified.
8.1.2 Verify the calibration of all measurement components (such as load cell and specimen deformation measurement device) of the testing system.

8.2 If any of the verifications yield data that does not comply with the accuracy specified, correct the problem prior to proceeding with testing.

9. Test Specimens

9.1 *Size* – Dynamic modulus testing shall be performed on test specimens cored from gyratory compacted mixtures. The average diameter of each test specimen shall be between 100 and 104 mm (3.94 and 4.09 in). The average height of each test specimen shall be between 147.5 and 152.5 mm (5.81 and 6.00 in).

9.2 *Aging* – Mixtures shall be aged in accordance with the 4-hours short-term oven aging procedure in AASHTO PP2.

9.3 *Gyratory Specimens* – Prepare 170 mm (6.69 in) high specimens to the required air void content in accordance with AASHTO T312.

Note 3 – Testing should be performed on test specimens (101.6 mm (4.00 in) diameter) meeting specific air void tolerances. The gyratory specimen (152.4 mm (6.00 in) diameter) air void content required to obtain a specified test specimen air void content must be determined by trial and error. Generally, the test specimen air void content is 1.5 to 2.5 percent lower than the air void content of the gyratory specimen when the test specimen is removed from the middle as specified in this test method.

9.4 *Coring* – Core the nominal 101.6 mm (4.00 in) diameter test specimens from the center of the gyratory specimens. Both the core drill and the gyratory specimen should be adequately supported to ensure that the resulting test specimen is cylindrical with sides that are smooth, parallel, and free from steps, ridges, and grooves.

9.5 *Diameter* – Measure the diameter of each test specimen at the mid height and third points along axes that are 90 degrees apart. Record each of the six measurements to the nearest 1 mm (0.04 in). Calculate the average and the standard deviation of the six measurements. If the standard deviation is greater than 2.5 mm (0.01 in) discard the specimen. For acceptable specimens, the average diameter, reported to the nearest 1 mm (0.04 in), shall be used in all material property calculations.

9.6 *End Preparation* – The ends of all test specimens shall be smooth and perpendicular to the axis of the specimen. Prepare the ends of the specimen by sawing with a single or double bladed saw. The prepared specimen ends shall meet the tolerances described below. Reject test specimens not meeting these tolerances.

9.6.1 The specimen ends shall have a cut surface waviness height within a tolerance of ± 0.05 mm (0.002 in) across any diameter. This requirement shall be checked in a minimum of three positions at approximately 120° intervals using a straight edge and feeler gauges approximately 8 - 12.5 mm (0.32 - 0.49 in) wide or an optical comparator.

9.6.2 The specimen end shall not depart from perpendicular to the axis of the specimen by more than 1 degree This requirement shall be checked on each specimen using a machinists square and feeler gauges.

9.7 *Air Void Content* – Determine the air void content of the final test specimen in accordance with AASHTO T269. Reject specimens with air voids that differ by more than 0.5 percent from the target air voids.

Note 4 – Considerable time can be saved if the cored test specimens were treated as wet, and the weights in water and saturated surface dry were measured immediately or within a short time period after coring. The test specimens can then be left to dry overnight, the dry weight can be measured the next day, and then they can be immediately prepared for testing.

9.8 *Replicates* – The number of test specimens required depends on the number of axial strain measurements made per specimen and the desired accuracy of the average dynamic modulus. Table 2 summarizes the replicate number of specimens that should be tested to obtain a desired accuracy limit (e.g., less than ±15 percent).

Table 2. Recommended Number of Specimens

LVDTs per Specimen	Number of Specimens	Estimated Limit of Accuracy
2	2	18.0
2	3	15.0
2	4	13.4
3	2	13.1
3	3	12.0
3	4	11.5

9.9 *Sample Storage* – If test specimens will not be tested within 24 hours, wrap specimens in polyethylene and store in an environmentally protected storage area at temperatures between 5 and 26.7°C (40 and 80°F).

Note 4 – To eliminate effects of aging on test results, it is recommended that specimens be stored no more than two weeks prior to testing.

10. Test Specimen Instrumentation

10.1 Attach mounting studs for the axial LVDTs to the sides of the specimen with epoxy cement. Figure 3 shows details of the mounting studs and LVDT mounting hardware. A detailed drawing of the LVDT mounting hardware that is currently in use is shown in Attachment A.

Note 5 – Quick setting epoxy such as Duro Master Mend Extra Strength Quick Set QM-50 has been found satisfactory for attaching studs. Additional guidance for stud alignment is outlined in Attachment B.

10.2 The gauge length for measuring axial deformations shall be 101.6 mm ±1 mm (4.00 in ± 0.04 in). Suitable alignment and spacing fixture shall be used to facilitate mounting of the axial deformation measuring hardware. The gauge length is measured between the stud centers

11. Procedure

11.1 The recommended test series for the development of master curves for use in pavement response and performance analysis consists of testing at –10, 4.4, 21.1, 37.8, and 54.4 ^{o}C (14, 40, 70, 100 and 130^{o}F) at loading frequencies of 0.1, 0.5, 1.0, 5, 10, and 25 Hz at each temperature. Each test specimen, individually instrumented with LVDT brackets, should be tested for each of the 30 combinations of temperature and frequency of loading starting with the lowest temperature and proceeding to the highest. Testing at a given temperature should begin with the highest frequency of loading and proceed to the lowest.

11.2 Place the test specimen in the environmental chamber and allow it to equilibrate to the specified testing temperature ± 1°F. A dummy specimen with a thermocouple mounted at the center can be monitored to determine when the specimen reaches the specified test temperature. In the absence of the dummy specimen, minimum recommended equilibrium temperature times are provided as a guideline.

Table 3. Recommended Equilibrium Times.

Specimen Temperature, ^oC (^oF)	Time from room temperature, hrs 25 °C (77 °F)	Time from previous test temperature, hrs
-10 (14)	overnight	-
4.4 (40)	overnight	4 hrs or overnight
21.1 (70)	1	3
37.8 (100)	2	2
54.4 (130)	2	1

** Note that the temperature equilibrium times may vary depending on the type of environmental chamber in use. Some testing laboratories reported as much as 6 hours to reach the equilibrium temperature.*

11.3 Place one of the friction reducing end treatments on top of the hardened steel disk at the bottom of the loading frame. Place the specimen on top of the lower end treatment, and mount the axial LVDTs to the hardware previously attached to the specimen. Adjust the LVDT to near the end of its linear range to allow the full range to be available for the accumulation of compressive permanent deformation.

11.4 Place the upper friction reducing end treatment and hardened steel disk on top of the specimen. Center the specimen with the hydraulic load actuator visually in order to avoid eccentric loading. Allow a time period for the test specimen to reach the test temperature equilibrium. (This time period may vary between 10 and 30 minutes after changing and reconnecting the next test specimen).

11.5 Apply a contact load (P_{min}) equal to 5 percent of the dynamic load that will be applied to the specimen.

11.6 Adjust and balance the electronic measuring system as necessary.

11.7 Apply sinusoidal (haversine) loading ($P_{dynamic}$) to the specimen in a cyclic manner. The dynamic load should be adjusted to obtain axial strains between 50 and 150 microstrain.

Note 6 – The dynamic load depends upon the specimen stiffness and generally ranges between 15 and 2800 kPa (2 and 400 psi). Higher load is needed at colder temperatures. Table 4 presents typical dynamic stress levels based on temperature.

Table 4. Typical Dynamic Stress Levels

Temperature, ^{o}C (^{o}F)	Range, kPa	Range, psi
-10 (14)	1400 - 2800	200 - 400
4.4 (40)	700 - 1400	100 - 200
21.1 (70)	350 - 700	50 - 100
37.8 (100)	140 - 250	20 - 50
54.4 (130)	35 - 70	5 - 10

11.8 Test the specimens from lowest to highest temperature; that is from -10 ^{o}C (14 ^{o}F) to 54.4 ^{o}C (130 ^{o}F). At each temperature apply the loading from highest to lowest frequency; that is from 25 Hz to 0.1 Hz. At the beginning of testing, precondition the specimen with 200 cycles at 25 Hz. Then load the specimen as specified in Table 5. A typical rest time period between each frequency run is 2 minutes. This rest period shall not exceed 30 minutes for any two-frequency runs.

Table 5. Number of Cycles for the Test Sequence.

Frequency (Hz)	Number of Cycles
25	200
10	200
5	100
1	20
0.5	15
0.1	15

11.9 At the end of any testing period, if the cumulative un-recovered deformation was found to be greater than 1500 micro units of strain, keep the test data up to this last testing period and discard the specimen. Use a new specimen for the rest of the testing periods. The loading stress level should be reduced by fifty percent.

12. Calculations

12.1 Determine the average amplitude of the sinusoidal load from the load cell and deformation measured from each axial LVDT over the last 5 loading cycles for each test condition.

12.2 Determine the average lag time (t_i) between the peak load and the peak deformation from each LVDT over the last 5 loading cycles for each test condition.

Note 7 – Different approaches are available to determine these. The approach is highly dependent upon the number of data points collected per cycle. Approaches that have been used include peak search algorithms, various curve fitting techniques, and Fourier Transform

12.3 Over the last 5 loading cycles and for each test condition, calculate the loading stress, σ_o, as follows:

$$\sigma_o = \frac{\overline{P}}{A}$$

Where:

$\overline{P}$ = average peak load
A = area of specimen
σ_o = average peak stress.

12.4 Over the last 5 loading cycles and for each test condition, calculate the recoverable axial strain individually for each LVDT, ε_o, as follows:

$$\varepsilon_o = \frac{\overline{\Delta}}{GL}$$

Where:

$\overline{\Delta}$ = average peak deformation
GL = gage length
ε_o = average peak strain

12.5 Over the last 5 loading cycles and for each test condition, calculate the dynamic modulus, |E*| individually for each LVDT as follows:

$$Dynamic\ Modulus, |E^*| = \frac{\sigma_o}{\varepsilon_o}$$

12.6 Over the last 5 loading cycles and for each test condition, calculate the phase angle individually for each LVDT:

$$\phi = \frac{t_i}{t_p} * (360)$$

Where:

t_i = average lag time between a cycle of stress and a cycle of strain (sec)
t_p = average time for a stress cycle (sec)

13. Master Curve Development

13.1 The mechanical behavior of viscoelastic materials such as asphalt mixtures is dependent on the temperature and time of load (frequency) at which the material is tested. In order to compare test results of various mixes, it is important to normalize one of these variables. Data collected at different temperatures can be "shifted" relative to the time of loading, so that the various curves can be aligned to form a single *master curve*.

13.2 The shift factor, a(T), defines the required shift (as log of time) at a given temperature, i.e., a constant by which the loading times must be divided to get a reduced time, t_r, for the master curve:

$$t_r = \frac{t}{a(T)}$$

Where:

t_r = reduced time, time of loading at the reference temperature
t = time of loading , the reciprocal of the loading frequency
$a(T)$ = shift factor as a function of temperature
T = temperature

The master curve development can be found in numerous documents on pavement materials characterization. The concept is illustrated in Figure 4, which presents the shifting of laboratory measured dynamic modulus test data to the reference temperature T_0 of 21.1 °C (70°F). A sigmoidal fitting function is used to construct the master curve.

13.3 Using the shift factors, the master curve can be constructed using a selected reference temperature of 70°F to which all data are shifted.

13.4 Various computer programs can be used to define relationships with a(T) and temperature. One method is to use the numerical optimization (Solver) provided in the Microsoft Excel program.

13.5 Different functions are used to mathematically model the material response and create the master curve for asphalt mixtures. For time or frequency dependency, the generalized power law is most widely accepted at low to intermediate temperatures. As higher temperature data is included, a polynomial and sigmoidal functions have been used. Caution should be exercised when employing polynomial fitting functions due to the polynomial swing in low and high temperatures, when extrapolating outside the range of data. The generalized power law and sigmoidal functions will approach asymptotically the limiting stiffness values, thus, allowing the prediction outside the measured range of data.

14. Report

14.1 For each individual LVDT report the dynamic modulus ($|E^*|$) and phase angle (ϕ) for each temperature-frequency combination tested.

14.2 Report the average peak stress (σ_o) and strain (ε_o) for each temperature-frequency combination tested.

14.3 Report, for each temperature-frequency combination tested, the dynamic modulus and phase angle for each replicate test specimen along with the average, standard deviation and coefficient of variation of the three replicates.

14.4 In addition, report the dynamic modulus replicate results in a format compatible with Table 6. This is the format of data entry required for the computer program "Asphalt Pavement Analysis and Design System" (APADS) that was developed under the 2002 Design Guide for the design of new and rehabilitated pavement structures.

14.5 Report the constructed master curve.

Table 6. Required Input Data for APADS 2002.

Temperature, °F	Replicate	Mixture |E*|, psi (or MPa) @ Frequency Noted					
		0.1	0.5	1	5	10	25
14	1						
	2						
	3						
	4						
40	1						
	2						
	3						
	4						
70	1						
	2						
	3						
	4						
100	1						
	2						
	3						
	4						
130	1						
	2						
	3						
	4						

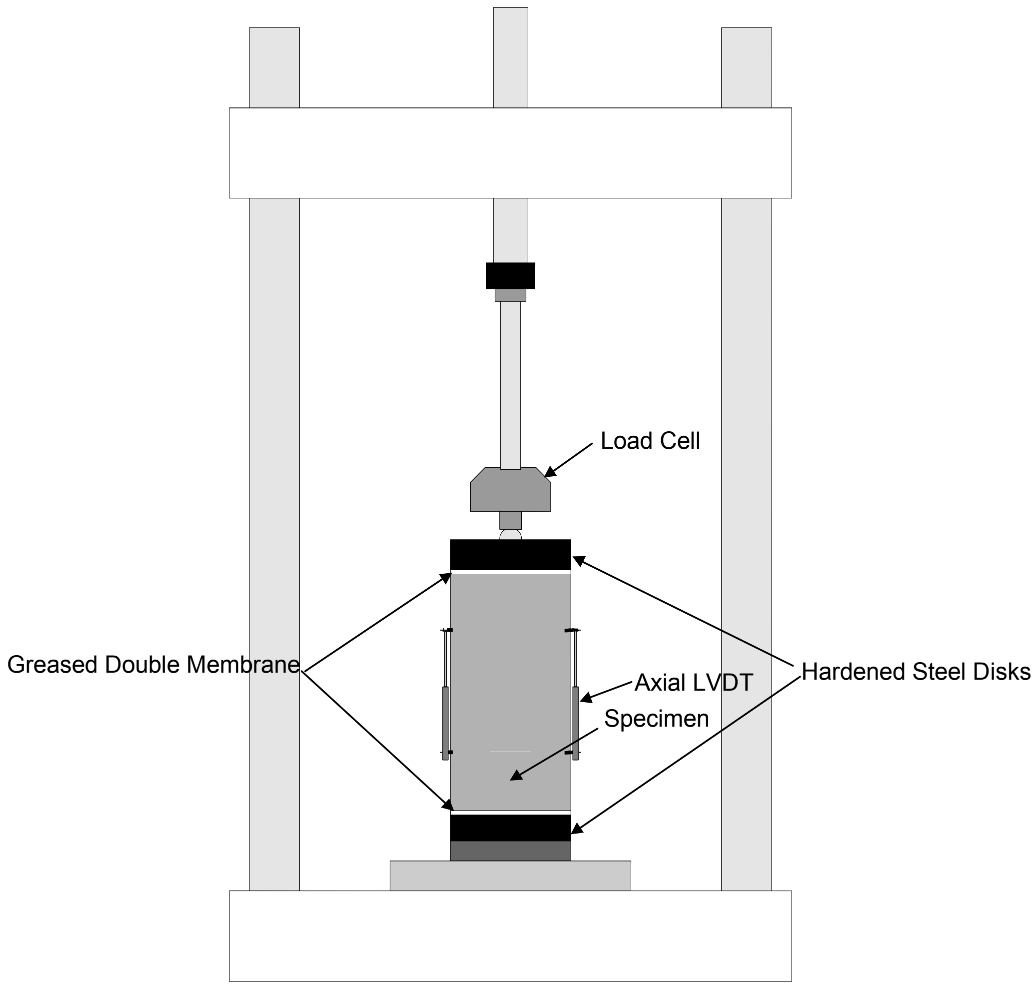

Figure 1. General Schematic of Dynamic Modulus Test.

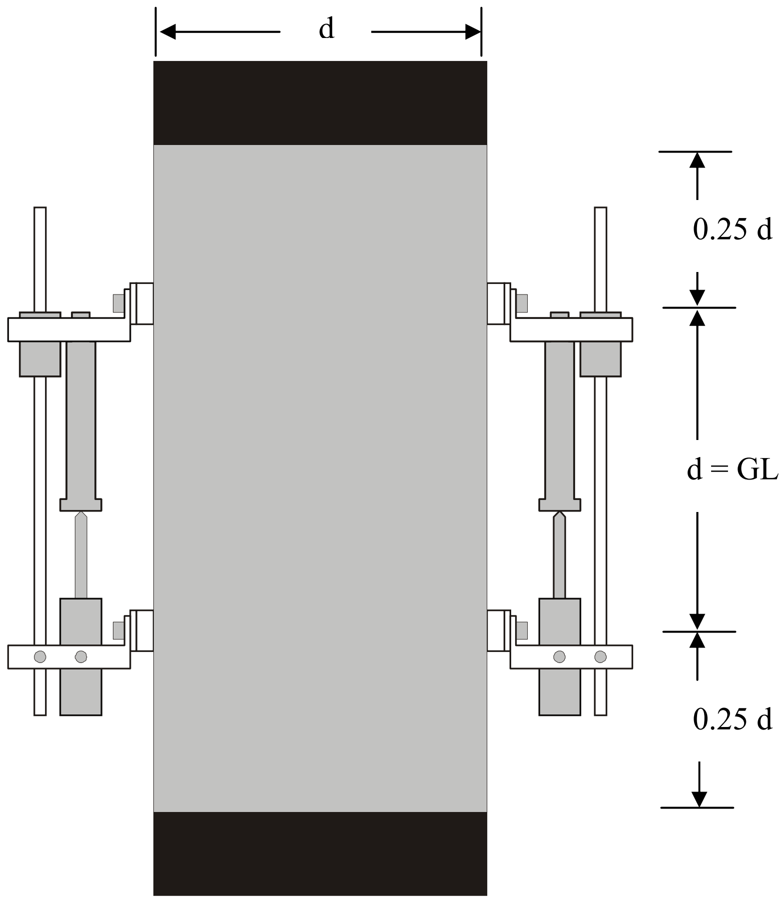

Figure 2. General Schematic of Gauge Points (*Not to scale*).

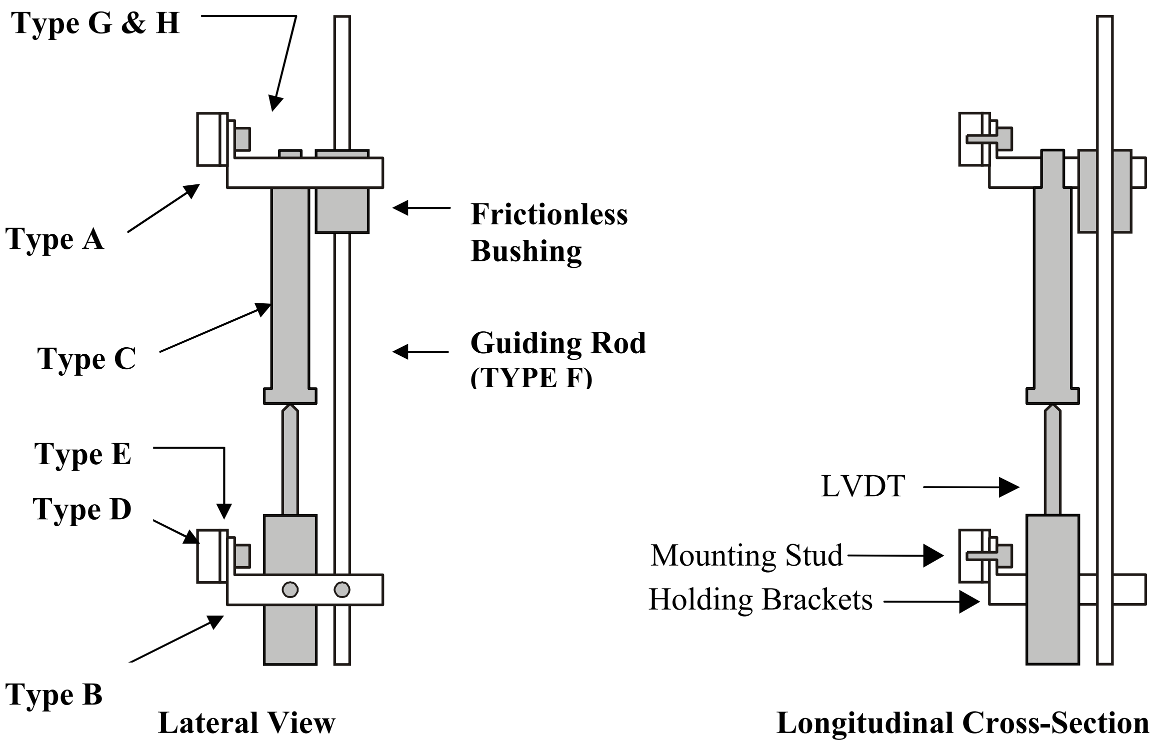

Figure 3. Mounting Hardware Details.
(See Attachment A for drawings details).

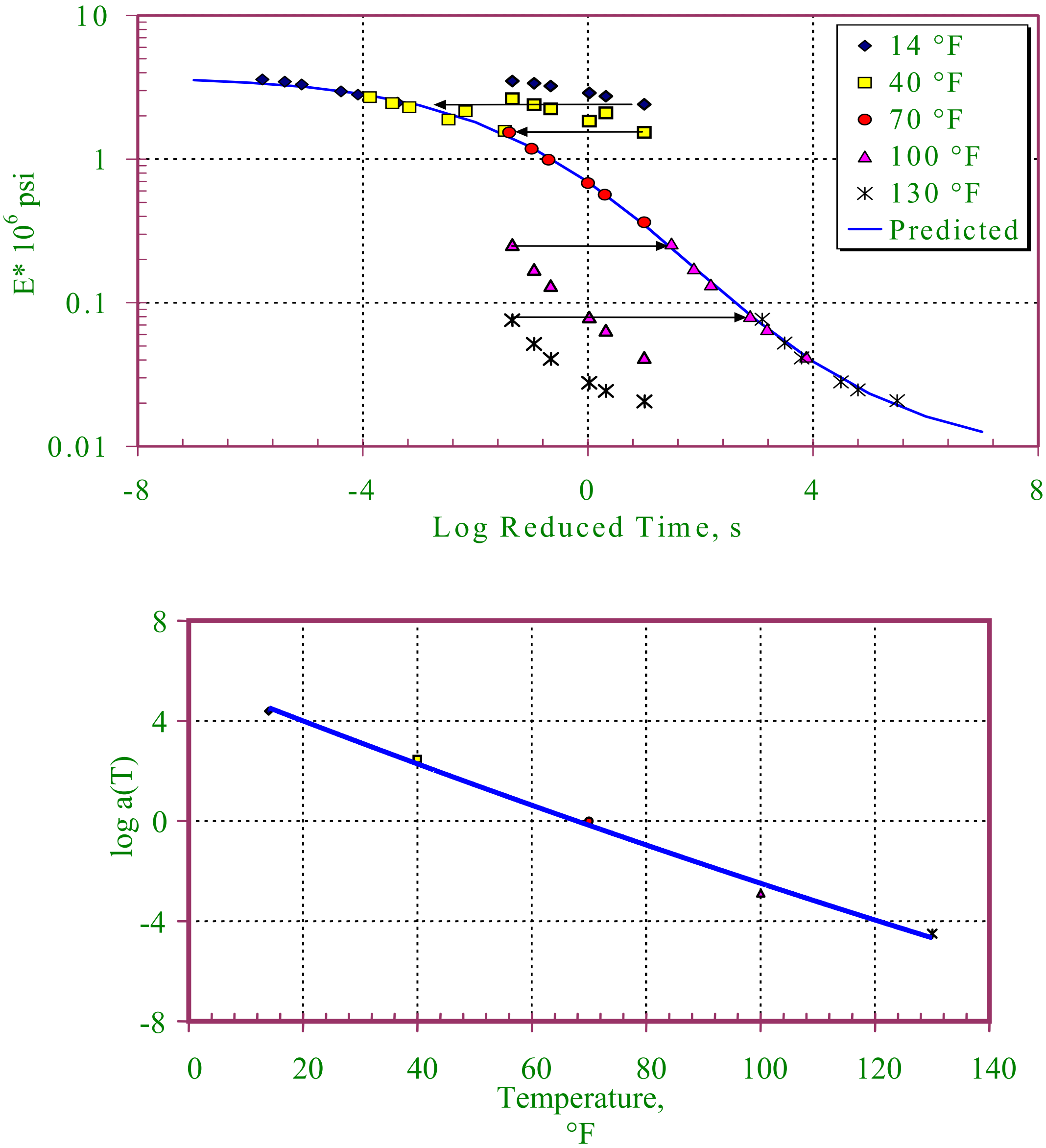

Figure 4. Example of Master Curve Construction.

ATTACHMENT A

LIST OF LVDT BRACKETS DETAILS USED BY ARIZONA STATE UNIVERSITY

LIST OF DRAWING ITEMS

- Type A Aluminum Bracket*
- Type B Aluminum Bracket*
- Type C Aluminum Bracket*
- Type D Brass Button
- Type E Brass Ring
- Type F Steel Bar
- Type G Screw (4-40 x ¼ cap screw)
- Type H Screw (4-40 x ¼ cap screw)
- Plastic Washer (4-40 plastic Washers)
- Super Ball Bushing Bearing, diameter 0.188 in, length 0.562 in**

NOTES

* Half of the screw holes are mirror images

** Bushing information

Description: Super Ball Bushing Bearing
Nominal Diameter: 0.188 in
Length: 0.562 in

Supplier: *MSC Industrial Supply Co*
555 W. Hoover, Suite #4
Mesa AZ 85210
Tel: 480-9641-500
1-888-203-5226, 1-800-645-7270

Catalog Number: 35-5-28009

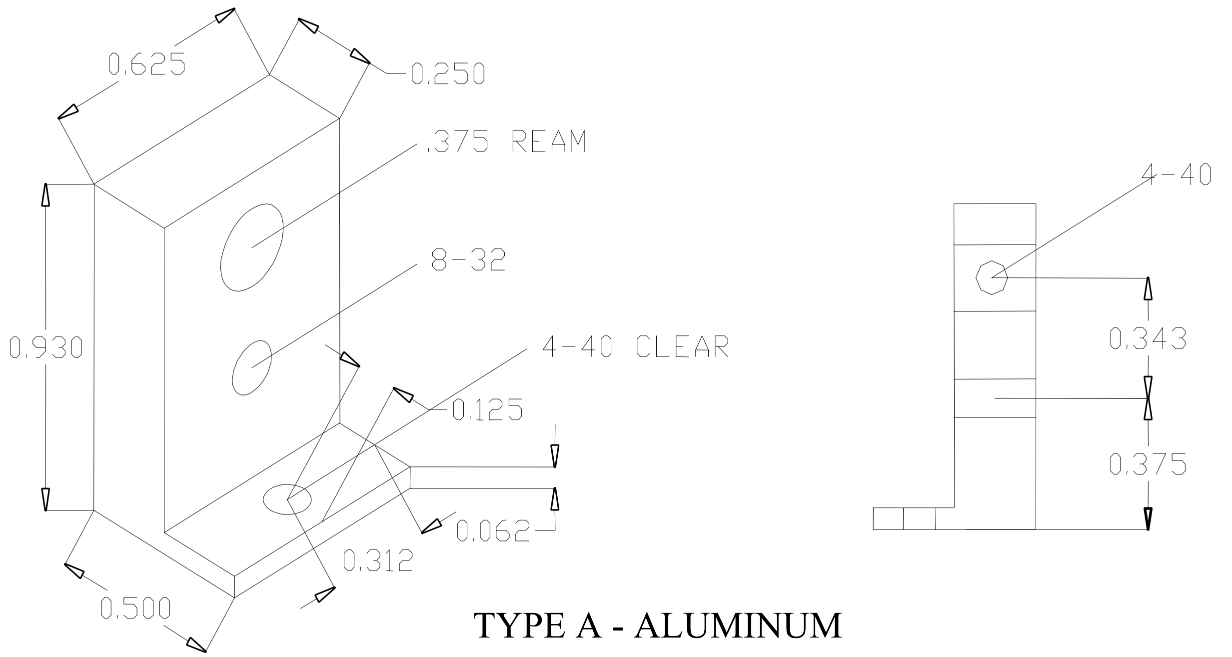

TYPE A - ALUMINUM

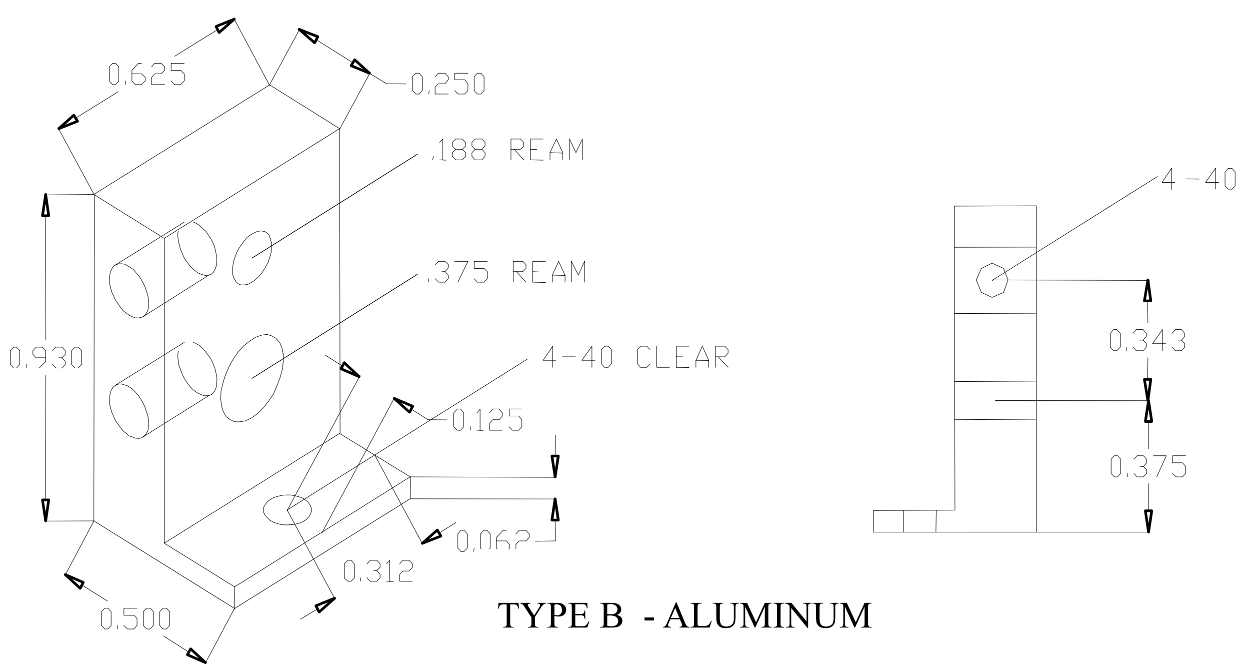

TYPE B - ALUMINUM

** All Units are in Inches*

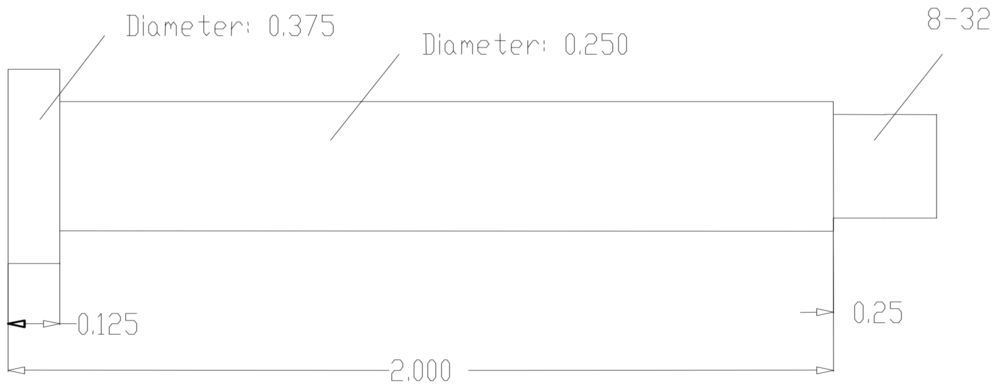

TYPE C - ALUMINUM

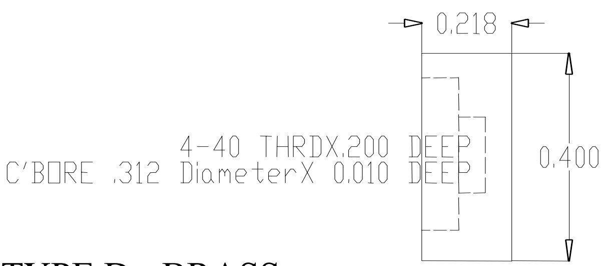

TYPE D - BRASS

TYPE F – STEEL

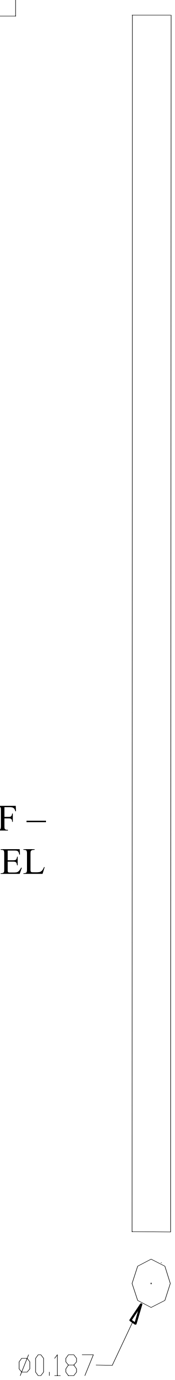

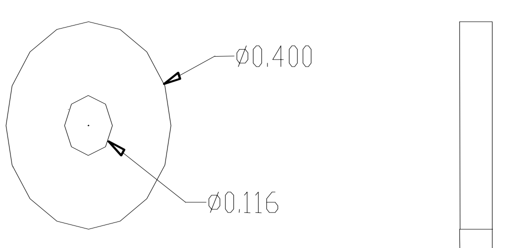

TYPE E - BRASS

** All Units are in Inches*

ATTACHMENT B

TEMPLATE FOR LOCATING MOUNTING PLUGS WHEN USING LVDT

The spacing and parallelism of the glued buttons is important when using the LVDT's. The figure below shows a simple flat metal bar with holes for the studs that hold the brackets. The bar must be flat and the holes exactly 101.6 mm (4 in) apart (25.4 mm (1 in) form each end). The holes should fit the studs closely. The mounting buttons are screwed to the bar and epoxy glue put on the buttons. Each bar is then lined up with an axial line on the specimen and two rubber bands put around as shown in Figure B-1. Keeping the rubber bands near the ends of the specimen permits applying all bars without waiting for glue to dry.

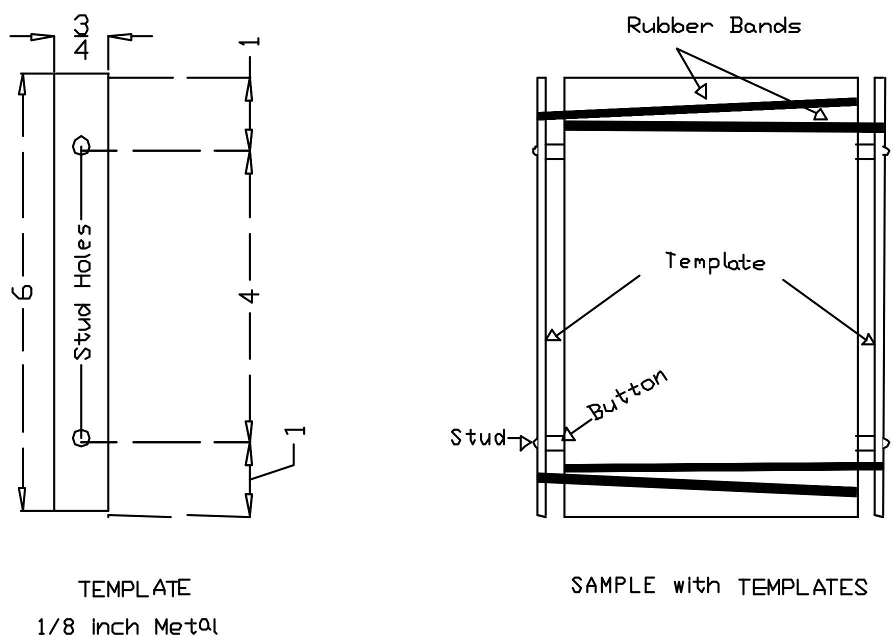

** All Units are in inches*

Figure B-1. Template for Locating LVDT Mounting Buttons.